AMPTIAC FORMAL REPORT

EURFNR - 534

EUR 3954 d.

UNITED STATES – EURATOM FAST REACTOR EXCHANGE PROGRAM

Original report number KFK 774

Title Creep Rupture Strength and Creep Behavior of Vanadium/Titanium and Vanadium/Titanium/Niobium Alloys

Author(s) H. Böhm, M. Schirra

Originating Installation Nuclear Research Center, Karlsruhe

Date of original report issuance June 1968

Reporting period covered

Translated from the original GERMAN

EURFNR - 534

KERNFORSCHUNGSZENTRUM

KARLSRUHE

June 1968

KFK 774
EUR 3954 d

Institute for Materials and Solids Research *)

Creep Rupture Strength and Creep Behavior of Vanadium/Titanium and Vanadium/Titanium/Niobium Alloys

H. Böhm, M. Schirra

OFFICIAL REPORT
USAEC-EURATOM
Fast Reactor Exchange

*) This work was carried out under the fast reactor Association concluded between the European Atomic Energy Community and the Gesellschaft für Kernforschung mbH, Karlsruhe.

Gesellschaft für Kernforschung mbH, Karlsruhe

1. Introduction

Increasing interest has recently been shown in vanadium alloys since a number of properties render them suitable as canning materials for fast reactors. The requirements imposed on a material used for these purposes are high creep rupture strength in the range 600 - 800°C, the minimum possible damage due to neutron irradiation at low absorption cross sections for fast neutrons, adequate resistance with respect to the coolant (sodium) and the fuel (uranium oxide or uranium carbide) and good workability.

→ p. 4

As compared with the austenitic steels planned to be used as canning materials in fast sodium-cooled breeder reactors, the vanadium alloys display a number of advantages justifying the interest in them. In the temperature range considered, for example, they have a much higher creep rupture strength (Ref. 1) than the high-temperature austenitic steels and, in particular, show no signs of high-temperature embrittlement due to neutron irradiation (Ref. 2). If metal fuel is used (uranium/plutonium/fissium alloys), the vanadium alloys are also clearly superior to the austenitic steels with regard to their compatibility with the fuel (Ref. 3). The corrosion behavior of the majority of vanadium alloys with respect to sodium is less good (Refs. 4 and 5), but promising development work is being conducted in this field. For helium-cooled fast reactors, vanadium alloys already constitute a suitable canning material since the corrosion problem largely no longer arises.

Important alloying elements for vanadium alloys have found to be titanium and niobium (increase in strength) as well as aluminum and chromium (improvement of resistance to corrosion). Despite the large number of alloys already tested, although these experiments largely consisted in screening tests, there is a widespread lack of systematic studies on the creep rupture strength and creep behavior of vanadium alloys, especially with regard to the long-time behavior.

Results concerning the creep rupture behavior of vanadium alloys have been elaborated by Rostoker and co-workers (Refs. 6 and 7) for vanadium alloys containing 40 - 60 % of titanium and additions of aluminum, chromium and carbon, while van Thyne and co-workers (Refs. 8 - 11) have obtained results for vanadium alloys with titanium contents of up to 20 % and niobium contents of 20 and 60 %. Studies were also carried out on the influence of carbon, nitrogen and boron with the aim of improving the heat resistance of the alloys by a finely distributed separation of solid phases. The strength values listed in the works mentioned mainly relate to fairly short residence times.

W. Pollack and co-workers (Ref. 12) report on a comprehensive program for the development of creep-resistant vanadium alloys. The aim was to increase the creep strength by the combination of solid solution hardening (via W, Mo, Cr, Ta, Nb, Ni, Fe, Ti, Al) and dispersion hardening (by the formation of carbides or nitrides of titanium and zirkonium). Alloys containing 8.5 % Cr, 9.9 % Ta, 1.24 % Zr and 0.05 % C and 9.1 % Cr, 3.3 % Fe, 1.3 % Zr and 0.05 % C were found to be particularly suitable.

The first results obtained by us from a systematic

study on the creep rupture strength and creep behavior of vanadium/titanium and vanadium/tinanium/niobium alloys were recently reported on (Ref. 1). The subsequent results are reported in the present work and a general account given of the creep rupture strength and creep behavior of this group of alloys.

2. Test Material

The studies were carried out on the alloys listed in Table 1. Together with vanadium, the alloy elements titanium and niobium form homogeneous solid solutions in the concentration ranges given. Owing to the interstitial impurities oxygen, nitrogen and carbon, the average content of which was about 600 ppm C, 1000 ppm O_2 and 400 ppm N_2, however, finely distributed oxide or carbide precipitations appear in the alloys.

The alloys were made by the Metallgesellschaft from the pure components, swaged into rods 8.5 to 10 mm in diameter and finally vacuum annealed for one hour at 900 - 950°C. The starting textures of the alloys studied are given in Figs. 1a - d.

The metallographic examination shows that annealing did not lead to a completely recrystallized texture in all the alloys, the alloys with a low titanium and a high niobium content displaying no or hardly any signs of incipient recrystallization. As the hardness measurements showed, however, a virtually complete removal of work hardening occurred in all of them. It is known that both in the case of pure vanadium (Ref. 13) and vanadium alloys (Ref. 14) large-scale recovery of the

mechanical properties is possible without recrystallization. The influence of the titanium on the recrystallization behavior is very marked, as can be seen from Figs. 1a - d (Ref. 1). Afterwards the recrystallization temperature drops with increasing titanium content above $\approx$ 3 % Ti. However, for the purposes of the studies, it appeared desirable to carry out the same annealing in all the alloys. Generally speaking it was found that the secondary creep rate $\dot{\varepsilon}$ is somewhat lower in alloys in the recrystallized state than after stress relief annealing. However, the heat treatment cannot influence the creep behavior solely via recovery and recrystallization, but also by changing the quantity and distribution of the carbide or oxide precipitations, which are clearly visible in the micrographs and have also been observed and identified by other authors (Ref. 3). The influence of the cold work and heat treatment on the creep rupture properties is to be discussed in a subsequent publication.

3. Experimental Procedure

The creep rupture and creep tests were carried out in vacuum creep test rigs at a pressure of $\approx 1 \times 10^{-5}$ torr (Fig. 2). Threaded samples 5 mm in diameter and 25 mm long were selected as the samples. In order to achieve a constant temperature over the entire length of the sample, it is surrounded with a shielding sheath. In long-time experiments (> 1000 h) the space between the sample and the sheath was filled with titanium swarf in order to preclude the possibility of surface oxidation by gettering. The test temperature was maintained constant to $\pm$ 2°C by three individually adjustable heating zones.

The sample elongation was measured continually during the test via the upper attaching bolts by means of gages or inductive recorders.

4. Test Results and Evaluation

4.1 Creep Rupture Strength

The studies aimed at determining the creep rupture strength of the alloys listed were carried out mainly at 650°C. In order also to obtain data on the long-time behavior or the alloys, the experiments were extended to residence times of up to > 10,000 hours.

The results of the studies, including the values published in a previous work, are listed in Figs. 3 - 6. Each figure contains the creep rupture curves for alloys with a constant niobium content and the titanium content as a parameter. The values confirm the results obtained previously on a much smaller number of alloys (Ref. 1), according to which the short-time strength at 650°C increases for rising titanium content, but the long-time strength drops.

A general picture of the creep rupture behavior of the V-Ti and V-Ti-Nb alloys is given in Figs. 7 - 9, which show specially the stresses for residence times of 100, 1000 and 10,000 hours. As can be seen from Fig. 7, the 100 hour creep rupture strength rises for increasing niobium and decreasing titanium content and in the concentration range studied reaches a maximum for 15 % of niobium and 3 % of titanium with a marked drop for lower titanium contents. The 1000 hour creep rupture strength (Fig. 8) shows the same dependence on the niobium content, but with regard to the titanium content

the strength maximum is extended to the range from 1 to 3 %. The values for $\sigma_{B/10000}$ (Fig. 9), which were extrapolated on the basis of the available results or interpolated from long-time studies now in progress ($>10{,}000$ hours), indicate that the strength peak is further displaced towards lower titanium contents (≈ 1 %) and the influence of the niobium content on the strength constantly decreases, at least in alloys with low titanium contents.

In addition to the studies at 650°C already mentioned, creep rupture values were also obtained for certain alloys at higher temperatures in order to provide an indication of the temperature-dependence of the creep rupture strength. For the binary alloys V-5Ti and V-20Ti the measured values are plotted in Figs. 10 and 11 together with the values for 650°C. It will be seen that, for decreasing titanium content, not only is the long-time behavior at 650°C improved, but also the creep rupture strength at higher temperatures. On ternary V-Ti-Nb alloys, only individual tests at temperatures of up to 920°C were carried out. With the exception of those for V-5Ti, the results are shown in Fig. 12. For purposes of extrapolation, the creep rupture strength values for certain alloys are plotted here versus the Larson-Miller parameter $P = T(C + \log t_B)$, with a value of 15 for the constant C.

As the results have shown, the V-Ti-Nb alloys can be regarded as decidedly temperature-resistant materials. The long-time behavior of the best V-Ti-Nb alloys corresponds to that of the sophisticated precipitation-hardening nickel alloys. Moreover, by the addition of small quantities of silicon it is possible to increase the creep rupture strength further and to achieve $\sigma_{B/1000}$ values of ≈ 70 kp/mm^2 at 650°C. As a result these

alloys are superior to all known materials with regard to their creep rupture behavior.

4.2 Creep Behavior

In order to obtain precise data on the creep behavior of the material it is necessary to determine the stress and temperature dependence of the secondary creep rate.

In many cases the stress and temperature dependence of the secondary creep rate $\dot{\varepsilon}$ can be satisfactorily described for low stresses by the formula (Refs. 15 and 16)

$$\dot{\varepsilon} = A \left(\frac{\sigma}{E}\right)^n e^{-Q_K/RT}$$

where Q_K is the activation energy of creep, n the so-called stress exponent, E the modulus of elasticity and A a structure-dependent factor. The activation energy Q_K is in many cases equal to the activation energy Q_D of the diffusion.

The activation energy which is normally determined from measurements of the creep rate at different temperatures on the basis of the equation

$$Q_K = R \frac{\Delta \ln \dot{\varepsilon}}{\Delta \frac{1}{T}}$$

deviates somewhat from the true activation energy Q_K, since no account is taken of the temperature-dependence of the modulus of elasticity.

The above formulae give the activation energies on the assumption that the stress exponent n is temperature-independent, which is to be expected in accordance with the theories of secondary creep, provided that no change occurs in the creep mechanism.

In a previous publication (Ref. 1), values for the activation energy of creep and of the stress exponent for various vanadium alloys for the temperature range 650 - 750°C were reported and briefly discussed. A noteworthy feature was the marked dependence of the activation energy on the titanium content as well as the values measured for high titanium contents were well above the values for the activation energy of diffusion. The very low activation energy found in vanadium alloys with $\approx$ 3 % of titanium, in conjunction with a relatively high stress exponent n, was found to be due to the fact that the creep processes in the temperature range studied are not diffusion-controlled. The results of this first investigation provided the impetus for carrying out more comprehensive measurements on a large number of binary V-Ti and ternary V-Ti-Nb alloys, the temperature range studied being extended to about $\approx$ 900°C.

The activation energy was determined in the familiar manner by measuring the creep rate $\dot{\varepsilon}$ of a sample under constant stress at different temperatures. The creep time at each temperature was about 70 - 100 hours before the temperature was rapidly raised by about 10°C in each case under stress. In a number of samples the temperature was alternately raised and lowered in order to detect possible changes in the creep rate as a result of texture modifications. In no case, however, was the creep rate found to have any influence which extended beyond the normal scatter range.

Figs. 13 - 17 give the temperature-dependence of the creep rate for the alloys whose creep behavior was studied over a wide temperature range. Since it is not possible to conduct the tests over the entire temperature range with one single stress, the creep rate curve shown in Figs. 13 - 17 is made up of several different sections which are displaced parallel in the direction of the ordinates and cover the creep rate range of 10^{-5} - 10^{-4}/hour for the particular stress. The activation energies of the creep given in the figures are thus valid for comparable creep conditions ($10^{-5} < \dot{\varepsilon} < 10^{-4}$/hour). As can be seen, the stress has no influence on the activation energy within the creep rate range taken as the basis.

It can be seen from the figures that the creep processes in the alloys containing 10 % and 20 % of titanium take place at a much higher activation energy at temperatures of below $\approx$ 700 - 720°C than at higher temperatures. A temperature-independent activation energy is found at 5 % of titanium, while for lower titanium contents the activation energy is lower at temperatures below 700°C than at higher temperatures.

In Fig. 18 the uncorrected activation energies obtained from measurements between 650 and 700°C are plotted for all the binary and ternary vanadium alloys studied as a function of the titanium content, the numerical values indicating the stresses at which the tests were carried out. The measurements confirm the results already published (Ref. 1) concerning the influence of the titanium on the activation energy of the creep in this temperature range and show again that the niobium content has no noticeable influence. A completely different dependence on the titanium content is shown by the activation energy at temperatures

of above 750°C (Fig. 19). Here there is only a very slight constant increase in the activation energy with the titanium content. The high activation energy of creep observed for titanium contents of 10 % and above is therefore limited to a narrow temperature range, the creep behavior at temperatures below 650°C still having to be determined.

The previous findings were confirmed with regard to the stress dependence of the creep rate. Figs. 20 - 23 give the creep rate $\dot{\epsilon}$ as a function of the stress for 650°C (and in some cases 700 and 800°C) for all the alloys studied. It was found that the dependence $\dot{\epsilon} = k \cdot \sigma^n$ is satisfactorily fulfilled in all cases. The stress exponent n obtained from Figs. 20 - 23 is given in Fig. 24 for the binary and ternary alloys as a function of the titanium content. Here the stress exponent shows a maximum for the test temperature of 650°C at low titanium contents, while the value for alloys with a higher titanium content is in the range to be expected with diffusion-controlled creep processes. As far as can be seen from the few results available, the maximum decreases for rising temperature. A reduction in the stress exponent for increasing temperature also occurs at higher titanium contents as can be seen from Fig. 24. Table 2 gives the n-values with the corresponding K-values for all the vanadium alloys studied.

While knowledge of the stress dependence and temperature dependence of the secondary creep rate is of decisive importance for understanding and explaining the processes which occur during creep, the creep limits provide an important characteristic for practical application which is determined by the creep behavior. For all the alloys studied, therefore, the 1 % and 2 % creep limits were determined from the creep curves, these being given in Figs. 25

- 29. Owing to the indirect elongation measurement via the attaching bolts, there is in some cases marked scatter of the 1 % limits in particular.

In order to be able to detect the influence of the titanium and niobium content on the ratio creep limit/creep rupture strength, Fig. 30 given the ratio $\sigma_{2/100}/\sigma_{B/100}$ and $\sigma_{2/1000}/\sigma_{B/1000}$ as a function of the titanium content. There is a clear reduction in the ratio for increasing titanium contents, but no marked influence of the niobium is to be observed.

4.3 Breaking Elongation

The breaking elongation measurements indicate that here, too, the titanium has a marked influence. The breaking elongation values measured during the creep rupture test at 650°C (Figs. 31 and 32) point to a clear pattern despite the scatter, which is in some cases severe. Whereas, for a titanium content of 3 %, the breaking elongation depends only very slightly on the holding time, it increases with the time for higher concentrations.

As is shown in the following section, the relatively marked increase in the breaking elongation with the holding time for higher titanium contents is related to incipient recrystallization. The alloys containing 3 and 5 % of titanium, on the other hand, show no signs of recrystallization even after very long holding times at 650°C, so that the dependence of the breaking elongation on the titanium content is doubtless connected with the influence which the titanium has upon the recovery and recrystallization behavior.

4.4 Metallographic studies *)

The metallographic studies were used to obtain more detailed data on the rupture behavior of the alloys and on the recrystallization phenomena which occur during the creep rupture test. The micrographs of the fracture zone of alloys V-2Ti-15Nb and V-5Ti given in Fig. 33 are characteristic of the rupture behavior. According to them the alloys studied show a transcrystalline fracture. At higher temperatures also the fracture is transcrystalline despite isolated intercrystalline incipient cracks (Fig. 34).

Knowledge of the rupture behavior of vanadium alloys is important with a view to their use as canning material in reactors, since the high-temperature embrittlement due to neutron irradiation rises as the tendency of the alloys towards intercrystalline fracture increases. In accordance with the rupture behavior results obtained, it was shown on a number of vanadium alloys (Ref. 2) that no high-temperature enbrittlement occurs in the temperature range of 600 - 750°C concerned.

It has already been pointed out that the recrystallization behavior of the vanadium alloys is to a large extent governed by the titanium content. While the recrystallization of cold-worked samples takes place between 850°C (for $\approx$ 20 % titanium and 50 % cold work) and 1000°C (for 3 % titanium and similar cold work), depending on the titanium concentration and cold work (Ref. 14), recrystallization processes occur at much lower temperatures during this creep test. In addition to a

---

*) The comprehensive metallographic studies were carried out by Mrs. Junge.

complete recrystallization with a generally speaking very fine-grained texture, one also observes serrated grain boundaries, which were also detected in other alloys (Refs. 17 - 19) during a creep study.

The metallographic studies conducted on numerous samples indicate that the occurrence of serrated grain boundaries can be regarded as a precursor of complete recrystallization, i.e., that it occurs at somewhat lower temperatures or lower deformations than the primary recrystallization. As Fig. 35 shows for a V-3Ti-20Nb alloy, for example, almost complete recrystallization is observed in the rupture zone. In the range outside necking, i.e., for lower deformation, predominantly serrated grain boundaries are found, while only the starting texture is found in the top section of the sample. Such grain boundaries occur at temperatures as low as 650°C in long-time creep tests even in alloys with a low titanium content, which are marked by a relatively high recrystallization temperature. The formation of new grains during primary recrystallization takes place both in the grain and at the severely serrated grain boundaries (Fig. 35).

Complete recrystallization during the creep rupture test is observed in alloys with titanium content of 20 % between 750 and 800°C (depending on the stress applied) and in alloys containing 3 - 5 % titanium at $\approx$ 850°C, i.e., the recrystallization temperature in the creep test is well below that determined on cold-worked samples.

Discussion of Test Results

The results obtained show clearly the marked influence which the titanium content of the

vanadium alloys has on the holding time t_B and the secondary creep rate $\dot{\varepsilon}$. For the discussion of the results it is important to know whether the dependence of the holding time on the titanium content is due solely to the dependence of the creep rate on the titanium content or whether the titanium also changes the holding time by influencing the rupture processes. The correlation between time and creep rate can generally be satisfactorily described by the equation

$$\log t_B + m \log \dot{\varepsilon} = K$$

where m (usually ≈ 1) and K are alloy-dependent quantities (Ref. 20). If the titanium content influences the time only via the creep rate, the quantities m and K should be independent of the titanium content, i.e., the values of $\dot{\varepsilon}$ and t_B should lie on one curve for all vanadium alloys. If allowances are made for the fairly marked scatter in the values of $\dot{\varepsilon}$ and t_B, it can be seen (Fig. 36) that the values for the various vanadium alloys lie within a scatter band. A precise analysis of the groups of values indicates that the holding time is reduced somewhat more slowly for increasing titanium content than should be the case if the holding time reduction were solely determined by the creep rate change. However, the difference is so slight that the holding time can be regarded as a function of the creep rate to a good approximation and hence the main stress in the discussions can be placed in the interpretation of the creep processes. If the activation energy and the stress exponent are first regarded as the quantities characterizing the creep process, then the values measured for the temperature range above 750°C are readily understandable.

The creep activation energies determined for this temperature range are in good agreement with those for the diffusion in pure vanadium and vanadium/titanium alloys, so it can be assumed with certainty that the creep at these temperatures is determined by the diffusion of vanadium and titanium and/or niobium atoms. A decision as to which diffusion process is the main one cannot be taken on the basis of the measured activation energies alone*), since no values are available for the diffusion of niobium in vanadium/titanium alloys. It is advisable to regard the climbing of dislocations as the process which determines the creep rate. The few stress exponent values measured for the temperature range above 750°C are in agreement with this. This provides further confirmation of the theory that the creep processes in body-centered cubic alloys are not fundamentally different from those in metals with high-density spherical systems, as Sherby (Ref. 21) and Vandervoort (Ref. 22) have already shown.

The creep processes at lower temperatures are much more complicated. The low activation energies and high stress exponents measured in the 650°C range for alloys with titanium contents of under 5 % suggest that the creep processes in this concentration and temperature range are not controlled by the diffusion of V, Ti or Nb atoms. Dislocation climbing can therefore not be regarded as a process which determines the rate.

On the basis of the available results it is not possible to decide which process determines

---

*) The values Q_K for the activation energy, which were corrected with allowances for the temperature-dependence of the modulus of elasticity, are only slightly below the indicated values of Q_K', so that no useful conclusions can be drawn from the corrected values either.

the creep is this concentration and temperature range. On account of the in some cases very low activation energies, which are within the range of values for the diffusion of interstitial impurities such as oxygen, nitrogen and carbon, it might at first be thought that dislocation blockage occurs owing to the elements listed, the creep process then being determined by the diffusion of the blocking atoms (Refs. 23 and 24). Apart from the fact that a much lower stress exponent would be to be expected in this case (Ref. 23), alloys have shown (Ref. 25) that no marked yield point occurs for titanium contents of below 5 %, i.e., the mechanism indicated.

While, in the case of low titanium alloys, it can hence be assumed that the creep behavior at 650°C is not diffusion-controlled, a diffusion-controlled creep process is likely at these temperatures in alloys with higher titanium contents (>10 %).

This is borne out if only by the fact that in these alloys marked recovery processes occur at the temperature under consideration, and, in the case of long-time creep tests, even incipient recrystallization is observed. The very high activation energy in this temperature range, however, does not permit such a simple explanation of the creep process as at higher temperatures.

It might first be assumed that the recrystallization which commences during creep simulates the very high activation energy, which, for example, is assumed to be the case with regard to the very high activation energy of creep in aluminum monocrystals. (Ref. 26). In this case one would expect a corresponding rise in the activation energy

even in alloys with lower titanium contents, although at higher temperatures. However, since none of the alloys studied with titanium contents of less than 10 % showed this increase in the activation energy, not even at temperatures at which a recrystallization occurs during the experiment, it can be broadly speaking assumed that the high value is not simulated by incipient recrystallization.

It is more likely that the causes are to be sought in an interaction between the oxygen atoms and the titanium atoms and dislocations. A factor militating in favor of this is that in the alloys studied only titanium, which possesses pronounced interactions with the interstitial impurities, exercises a marked influence upon the creep activation energy. Moreover, it is known (Ref. 25) that, contrary to what might be expected, a pronounced yield point due to interactions between interstitial impurities and dislocations occurs with high titanium contents, but not at low contents, so that the titanium probably does not completely react with the interstitially dissolved elements. The high activation energy may then possibly be ascribed to the dislocation blockage or the removal of this blockage. This assumption is borne out by the results of hot tensile tests on alloys containing 20 % of titanium at higher temperatures. It was found that a marked yield point occurs in this alloy only up to about 650°C, i.e., above this temperature there is no more dislocation blockage due to the interstitial impurities, while alloys containing 5 % of titanium (no yield point effect is observed below 5 %) display a marked yield point even at 850°C.

Similar behavior with regard to the activation energy of creep is shown by an aluminum

alloy containing 3.2 % of Mg, in which a marked rise in the activation energy was recorded in a narrow temperature range (Ref. 27). Here, too, dislocation blockage phenomena are regarded as a possible cause of the extreme activation energy value, in accordance with Cottrell's mechanism.

The available results, particularly those concerning the concentration-dependence of the creep parameters, provide initial indications of the possible processes involved, as has been shown, but it is not yet possible to obtain a precise and detailed explanation of the unexpected dependency of the creep rate and residence time on the titanium content. It would appear to be necessary here to study the influence of the content of interstitial impurities, which according to the remarks made above are of importance for the creep behavior. The fact that alloys made from different starting materials show no abnormal scatter suggests that there is noticeable relation between the creep behavior and the concentration of these elements for relatively high oxygen, nitrogen and carbon contents (together $> \approx$ 2000 ppm). However, tests are now being conducted to determine how the creep behavior changes for much lower contents of these elements.

Very little data are available either on the almost complete recovery of the vanadium alloys without recrystallization, which doubtless had a decisive influence upon the creep behavior. This is likely to be the reason for the unexpected creep behavior of cold-worked samples, in which breaking elongation values of $>$ 150 % were observed in the creep test. (Ref. 28). It is not yet possible to say to what extent the recovery processes are related to the content of interstitial impurities.

At creep temperatures of above 650 - 700°C (depending on the titanium content) the pure recovery processes are accompanied by grain boundary migration and recrystallization. The formation of serrated grain boundaries is particularly striking.

Since this form of grain boundary is not observed in the recrystallization of cold-worked vanadium samples but only during creep, its occurrence must be closely related to creep deformation. The marked increase in the grain boundary surface and hence in the boundary surface energy as a result of the formation of serrated grain boundaries indicates that there must be a strong driving force for grain boundary migration, which, on the basis of the average radius of curvature of the teeth in the grain boundaries, is found to be $\approx 10^7$ dyn/cm^2, a grain boundary energy of 1000 erg/cm^2 being assumed.

The fact that serrated grain boundaries only occur during creep, but not during recrystallization, can have various reasons. For example, deformation during creep at higher temperatures produces a different dislocation arrangement than at low temperatures and hence influences the grain boundary migration during recrystallization. Seen from this angle, the results obtained hitherto concerning the occurrence of serrated grain boundaries are also explained. It is assumed that a very pronounced sub-grain formation occurs in the region of the grain boundaries during creep in the event of grain boundary slip, where the size of the sub-grains on both sides of the grain boundary can differ considerably. In this case grain boundary migration in the direction of the small sub-grains would occur (strain-induced grain boundary movement), which may lead to the formation of grain boundaries described.

This mechanism can not be ruled out in the vanadium alloys either, especially since the marked recovery of the mechanical properties without recrystallization point to a pronounced sub-grain formation. An estimation shows that such a process is possible from the energy angle if the dislocation density of the migrating boundary is greater than about $10^{11}/cm^2$, a value which can readily be reached.

Moreover, however, it is conceivable that stress-induced grain boundary movement occurs as a result of the marked increase in the stresses effecting the grain boundaries due to the dislocation blockage. On the basis of the results obtained it is barely possible to decide which process (strain or stress-induced movement) is the decisive one. Long-time anneals on samples with serrated grain boundaries at 800 or 900°C without stress produced no change in the grain boundaries, so that it can be assumed that the formation of the grain boundaries is largely determined by the deformation processes which occur during grain boundary migration and less by a previously formed dislocation structure.

Abstract

Studies were performed on the creep rupture and creep behavior of binary V-Ti and ternary V-Ti-Nb alloys in the temperature range above 650°C.

The results show the prominent influence of the titanium on the creep rupture and creep behavior of the alloys. For titanium contents of above about 1 % the creep rupture →

strength drops for rising titanium concentrations, while the short-time high-temperature strength rises. This applies regardless of the niobium content. For increasing niobium contents the holding time is increased, but the influence of the niobium drops for rising holding times, so that the $\sigma_{B/10,000}$ values depend only slightly on the niobium content. The best vanadium alloys show long-time strength values which can barely be reached by any other materials. A marked dependence on the titanium content is also displayed by the creep activation energy in the temperature range around 650°C, while the niobium content has no influence upon this quantity.

The results of the studies indicate that the creep rupture and creep behavior of the alloys are also determined by the interactions between titanium and the interstitial impurities at high titanium contents.

References

1) H. Böhm und M. Schirra, J.Less-Common Metals, 12 (1967), 280

2) H. Böhm, W. Dienst, H. Hauck und H.J. Laue, ASTM Spec.Techn. Publ.

3) W. Burt et al., Argonne National Laboratory Reports ANL-6928 (1965) und ANL-7127 (1966)

4) "Alkali Metal Coolants", Symposium der IAEA, Wien 1967 S. 45 und S. 63

5) H.U. Borgstedt, G. Drechsler und G. Frees, Werkstoffe und Korrosion 18 (1967) 894

6) Armour Research Foundation, WADCTR 52-145:
W. Rostoker und M. Hansen, AD 13776, 1952;
W. Rostoker, D.J. McPherson und M. Hansen, AD 56083, 1964;
A.S. Yamamoto und W. Rostoker, AD 58609, 1955

7) W. Rostoker, A.S. Yamamoto und R.E. Riley, Trans.Am.Soc. Metals, 48 (1956) 560-78

8) K.F. Smith und R.S. Van Thyne, Argonne Nat.Lab., ANL-5661, W-31-109-eng-38, 1957

9) R.J. Van Thyne, in W.R. Clough, Reactive Metals, Interscience, New York/London, 1959, S. 403

10) B.R. Rajala und R.J. Van Thyne, Armour Research Foundation, Summary Rpt. 2165-6, AD 231512, NDas 59-6050-C, Dez. 1959

11) B.R. Rajala und R.J. Van Thyne, Armour Research Foundation, Final Rept. 2191-6, Dez. 1960

12) W. Pollack, E.C. Bishop, R.T. Begley und R.W. Buckman, Trans. ANS 10 (1967), 120

13) C.E. Lacy und C.J. Beck, Trans. ASM 48 (1956), 579

14) M. Rühle, persönl. Mitteilung

15) O.D. Sherby, Acta Met. 10 (1962), 135

16) C.R. Barrett, A.J. Ardell und O.D. Sherby, Trans. AIME 230 (1964), 200

17) A.W. Mullendore und N.J. Grant in "Structural Processes in Creep", Iron and Steel Institute, London, 1961, S. 44

18) H.C. Chang und N.J. Grant, Trans. AIME 194 (1952), 619

19) H. Brunner und N.J. Grant, Trans. AIME 218 (1960), 122

20) F.C. Monkman und N.J. Grant, Proc. ASTM 56 (1956), 593

21) O.D. Sherby, Acta Met. 10 (1962), 135

22) R.R. Vandervoort, Trans. AIME 242 (1968), 345

23) J. Weertman, J. Appl. Phys. 28 (1957), 1185

24) J. Weertman, Trans. AIME 218 (1960), 207

25) H. Böhm und F. Mir, J.Less-Common Metals 11 (1966), 408

26) Y.A. Rocher, L.A. Shepard und J.E. Dorn, Trans. AIME 215 (1959), 316

27) N.R. Borch, L.A. Shepard und J.E. Dorn, Trans. ASM 52 (1960), 494

28) H. Böhm und M. Schirra, Veröffentlichung demnächst

Table 1 : List of alloys studied

(in wt.%)

		V - 1 Ti - 15Nb	
		V - 2 Ti - 15Nb	
V - 3 Ti	V - 3 Ti - 10Nb	V - 3 Ti - 15Nb	V - 3 Ti - 20Nb
		V - 4 Ti - 15Nb	
V - 5 Ti	V - 5 Ti - 10Nb	V - 5 Ti - 15Nb	V - 5 Ti - 20Nb
	V - 7,5Ti- 10Nb	V - 7,5 Ti - 15Nb	V - 7,5 Ti - 20Nb
	V - 10 Ti- 10Nb	V - 10 Ti - 15Nb	V - 10 Ti - 20Nb
V - 20 Ti	V - 20 Ti- 10Nb		V - 20 Ti - 20Nb

Table 2 : List of n- and k-values of alloys studied

Alloy	Test temperature	n	k	Alloy	Test temperature	n	k
V - 3Ti	650°	10,3	$3,6 \cdot 10^{-21}$	V-1Ti-15Nb	650°	11,3	$1,8 \cdot 10^{-23}$
V - 5Ti	650	9,0	$4,6 \cdot 10^{-17}$	V-2Ti-15Nb	650	7,4	$2,7 \cdot 10^{-16}$
V - 5Ti	700	4,7	$8,6 \cdot 10^{-11}$	V-3Ti-15Nb	650	6,6	$3,7 \cdot 10^{-15}$
V - 20Ti	650	4,2	$7,4 \cdot 10^{-12}$	V-4Ti-15Nb	650	5,6	$3,8 \cdot 10^{-13}$
V - 20Ti	700	2,9	$3,1 \cdot 10^{-7}$	V-5Ti-15Nb	650	5,3	$2 \cdot 10^{-12}$
V - 20Ti	800	1,9	$3,9 \cdot 10^{-5}$	V-7,5Ti-15Nb	650	4,5	$1,5 \cdot 10^{-10}$
V-3Ti-10Nb	650	6,4	$1,3 \cdot 10^{-14}$	V-10Ti-15Nb	650	3,9	$3,5 \cdot 10^{-9}$
V-5Ti-10Nb	650	5,5	$1,4 \cdot 10^{-12}$	V-3Ti-20Nb	650	8,1	$9,3 \cdot 10^{-18}$
V-7,5Ti-10Nb	650	4,4	$4,6 \cdot 10^{-10}$	V-5Ti-20Nb	650	6,9	$3,4 \cdot 10^{-15}$
V-10Ti-10Nb	650	3,4	$2,0 \cdot 10^{-8}$	V-7,5Ti-20Nb	650	4,7	$5,5 \cdot 10^{-11}$
V-20Ti-10Nb	650	3,1	$4,0 \cdot 10^{-7}$	V-10Ti-20Nb	650	6,2	$1,1 \cdot 10^{-13}$
				V-20Ti-20Nb	650	4,6	$2,4 \cdot 10^{-10}$

Bild 1a

V-3Ti

HV_{30} = 174-184

V-5Ti

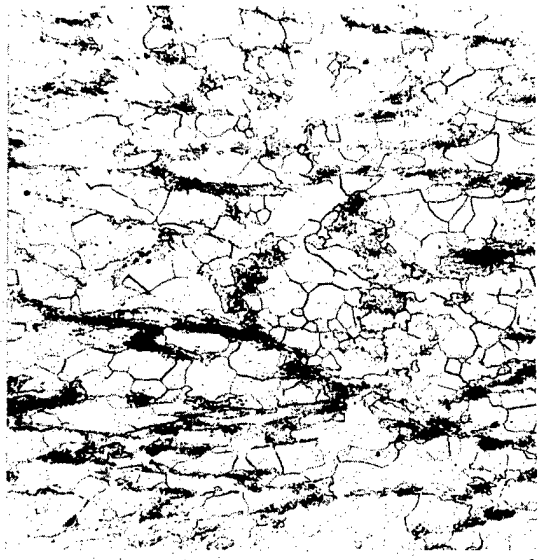

HV_{30} = 136

V-1Ti-15Nb

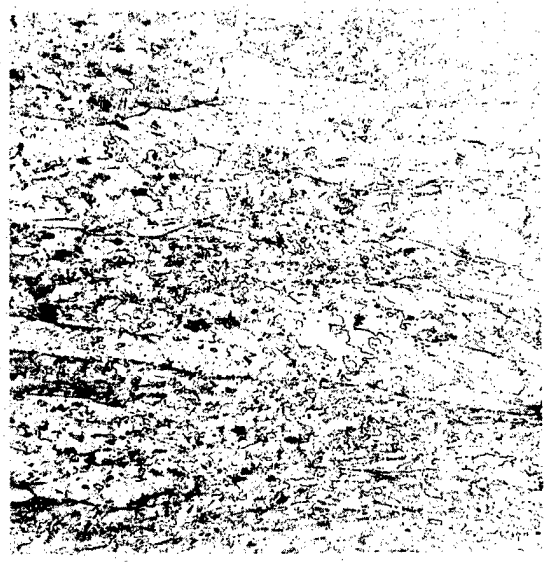

HV_{30} = 242-269

Ausgangsgefüge

Zustand 900-950° 1h Vakuum

Ätzung: Glyzerin: HF : HNO_3
3 : 2 : 1

These photographs reduced 10% in printing process.

V = x 100

Bild 1b

V-2OTi

HV_{30} = 197-202

V-3Ti-1ONb

HV_{30} = 244

V-2Ti-15Nb

HV_{30} = 242-250

V-3Ti-15Nb

HV_{30} = 288

V-3Ti-20Nb

HV_{30} = 288 x 100

These photographs reduced 10% in printing process.

Bild 1c

V-5Ti-10Nb

HV_{30} = 244

V-7,5Ti-10Nb

HV_{30} = 230-250

V-4Ti-15Nb

HV_{30} = 239-242

V-5Ti-15Nb

HV_{30} = 249-260

V-5Ti-20Nb

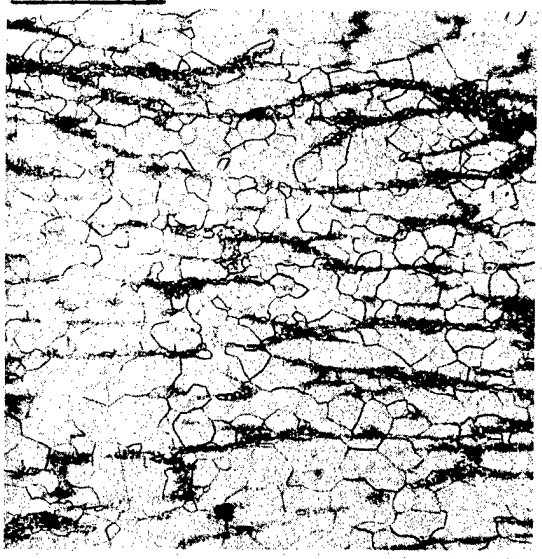

HV_{30} = 230-237

V-7,5Ti-20Nb

HV_{30} = 271-277

These photographs reduced 10% in printing process.

x 100

Bild 1d

V-10Ti-10Nb

HV_{30} = 216-226

V-20Ti-10Nb

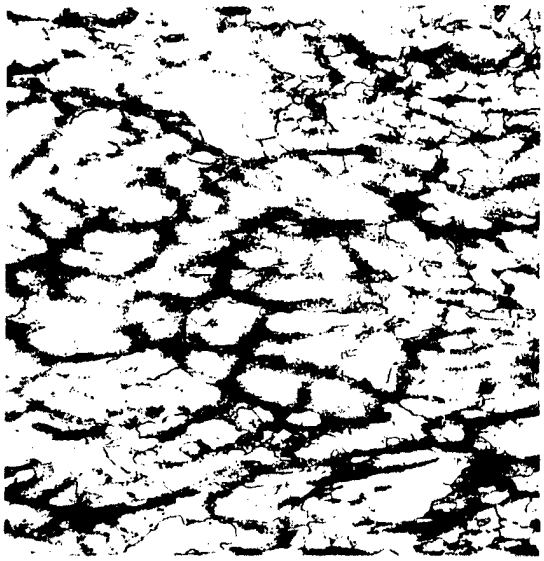

HV_{30} = 230-250

V-7,5Ti-15Nb

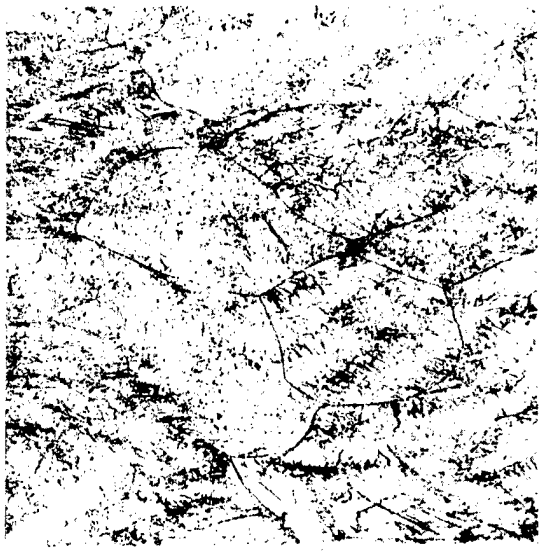

HV_{30} = 256

V-10Ti-15Nb

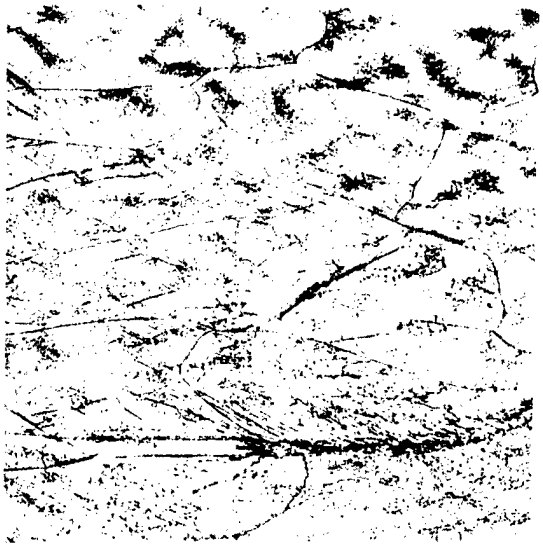

HV_{30} = 252-257

V-10Ti-20Nb

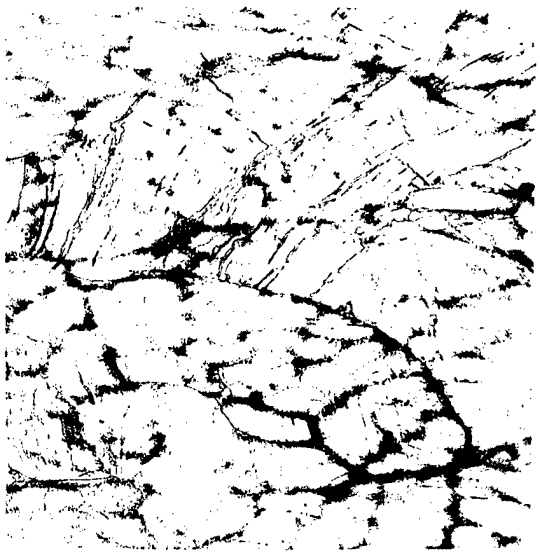

HV_{30} = 275-283

V-20Ti-20Nb

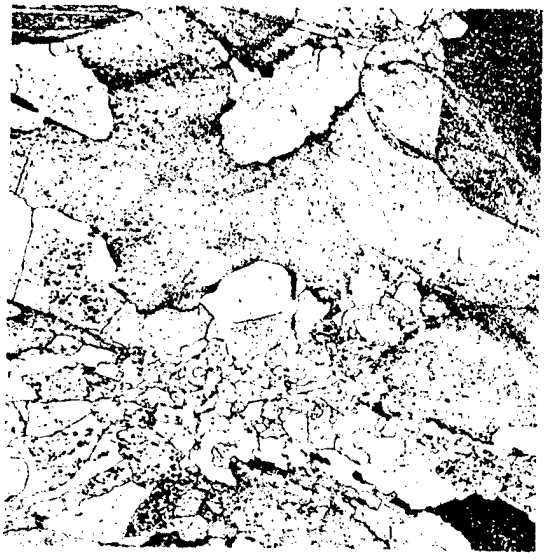

HV_{30} = 257-260

x 100

These photographs reduced 10% in printing process.

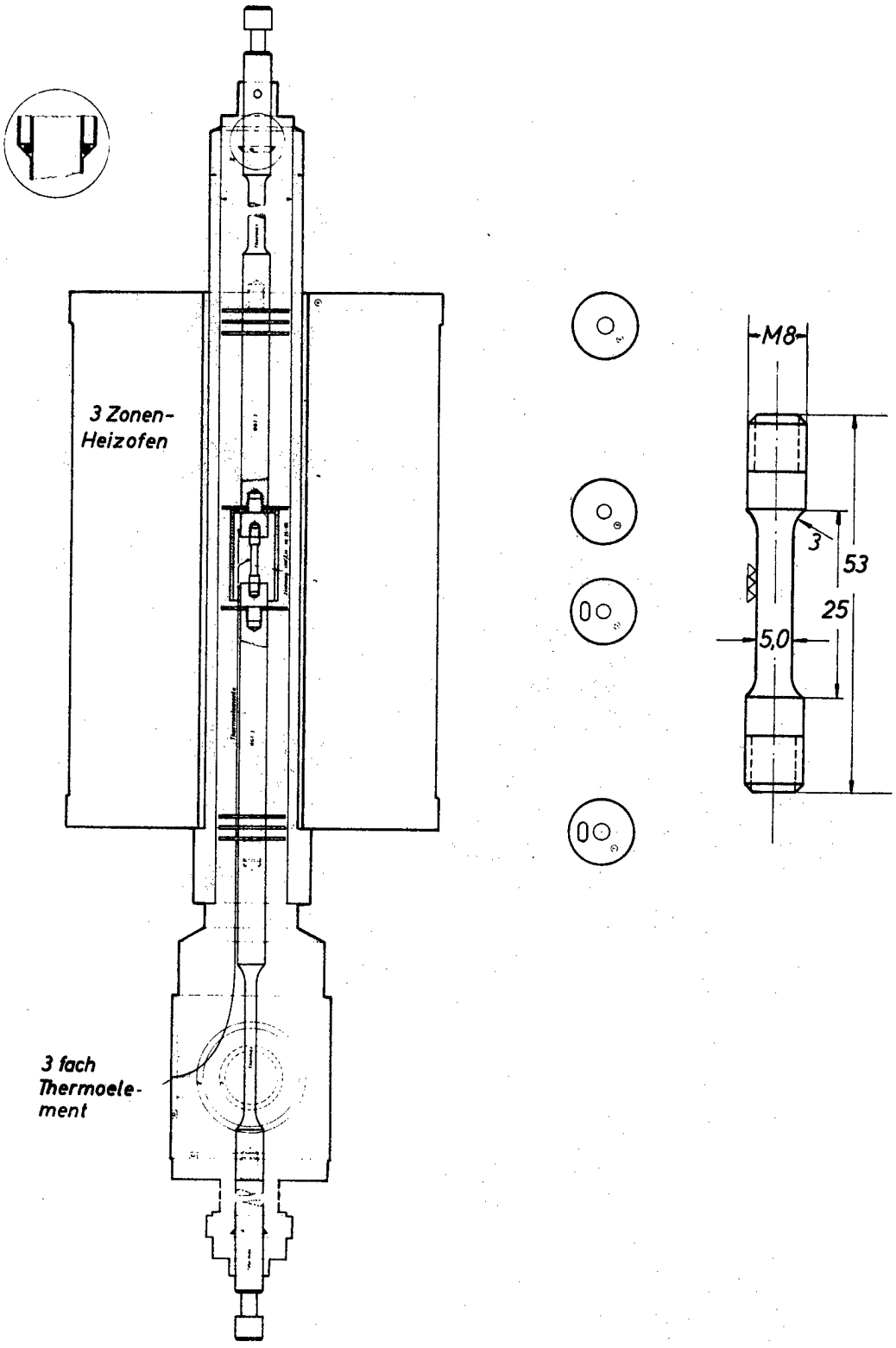

Bild 2: Probenform und Teststrecke für Vakuum-Zeitstandversuche

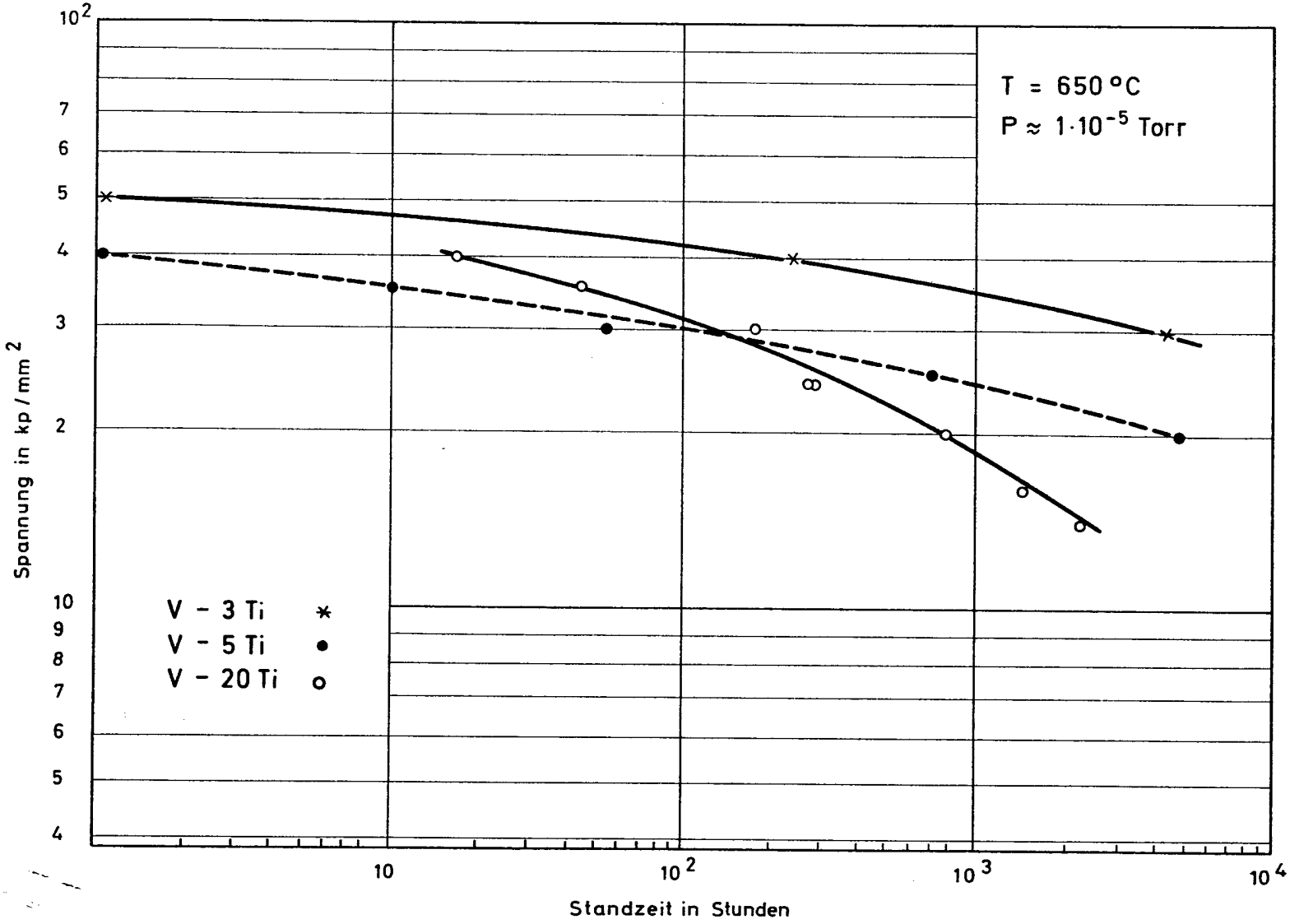

Bild 3: Einfluß des Ti-Gehaltes auf die Zeitstandfestigkeit von V-Legierungen

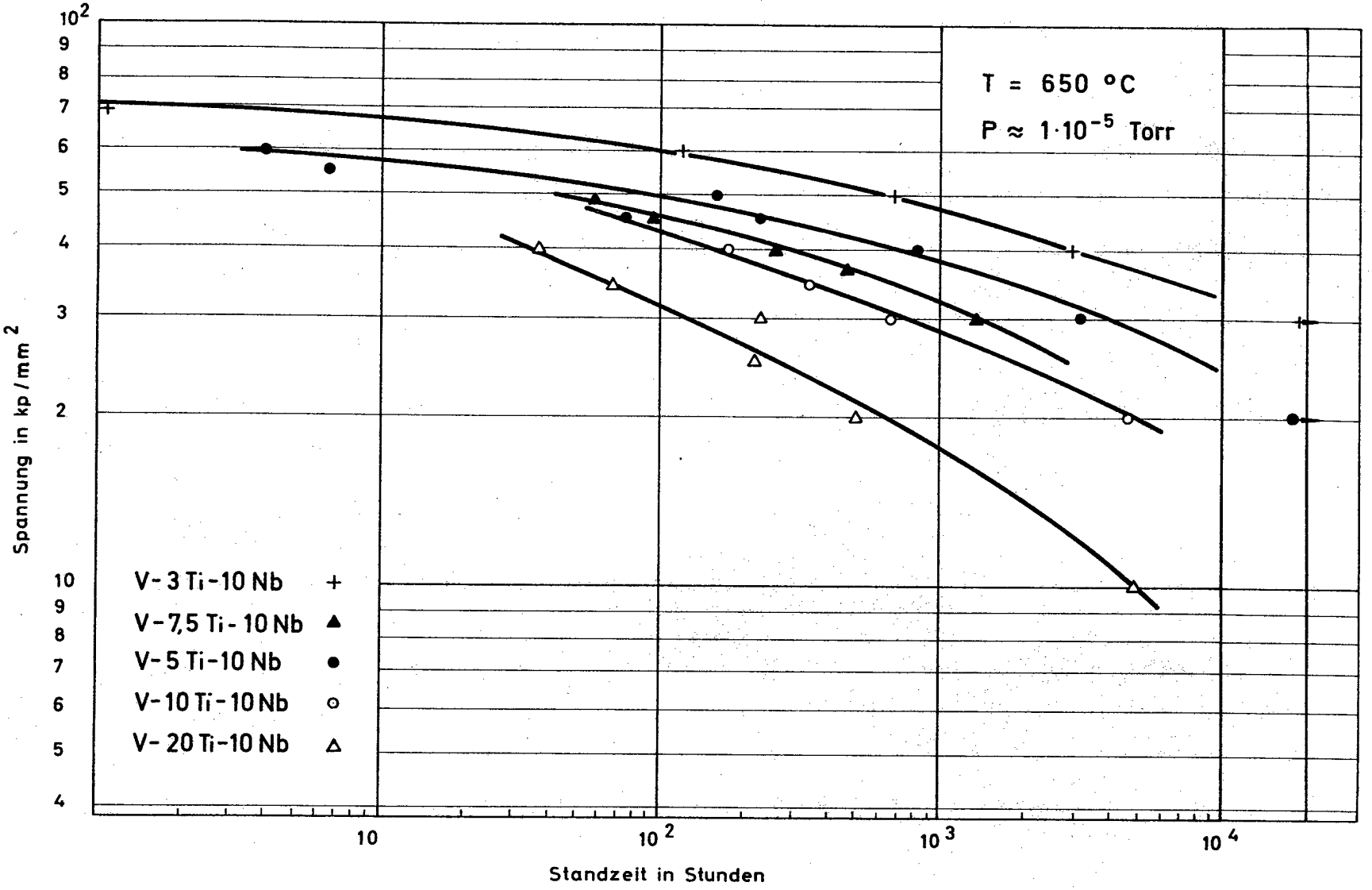

Bild 4: Einfluß des Ti-Gehaltes auf die Zeitstandfestigkeit von V-10Nb-Legierungen

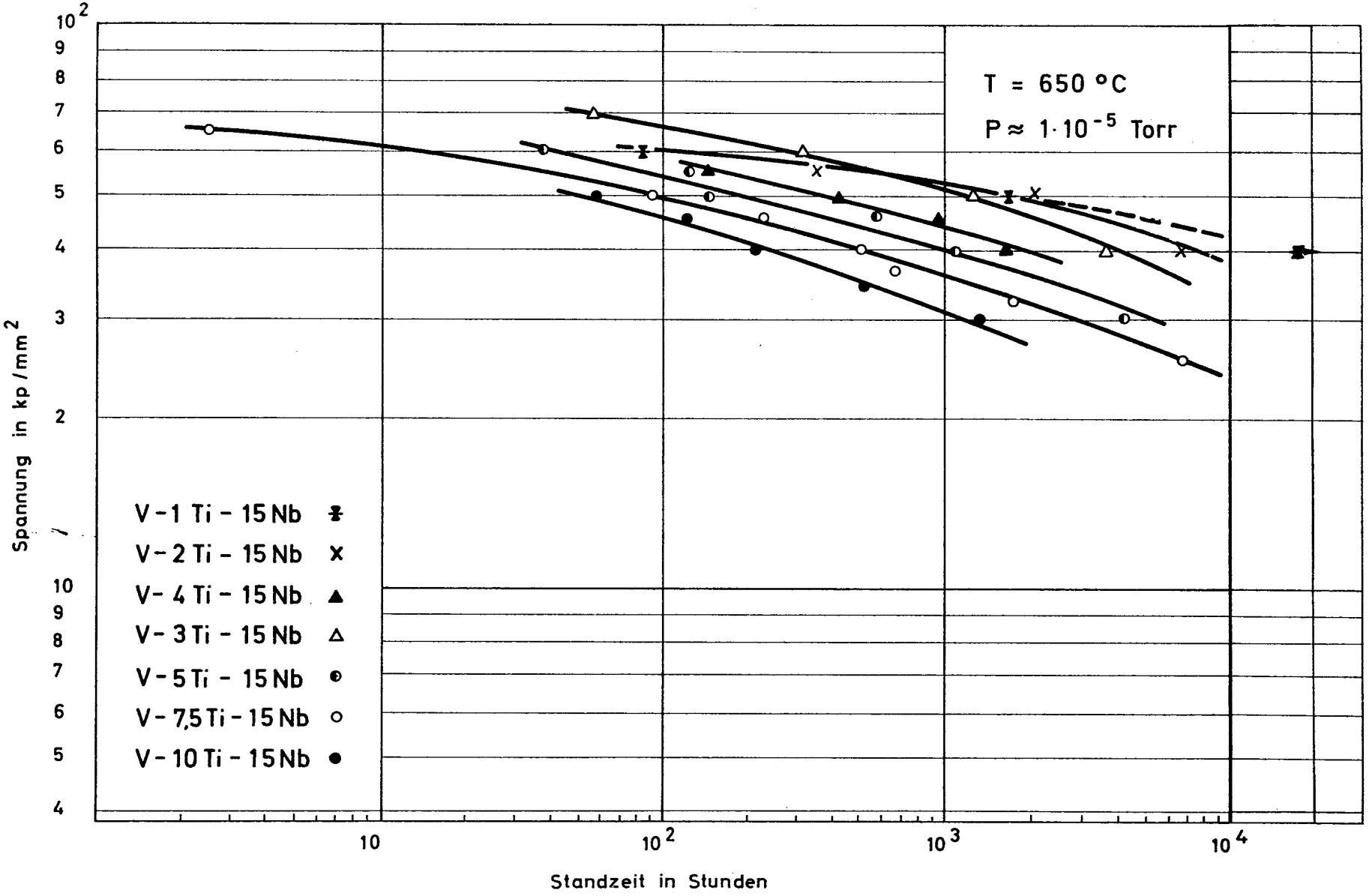

Bild 5 : Einfluß des Ti-Gehaltes auf die Zeitstandfestigkeit von V-15 Nb - Legierungen

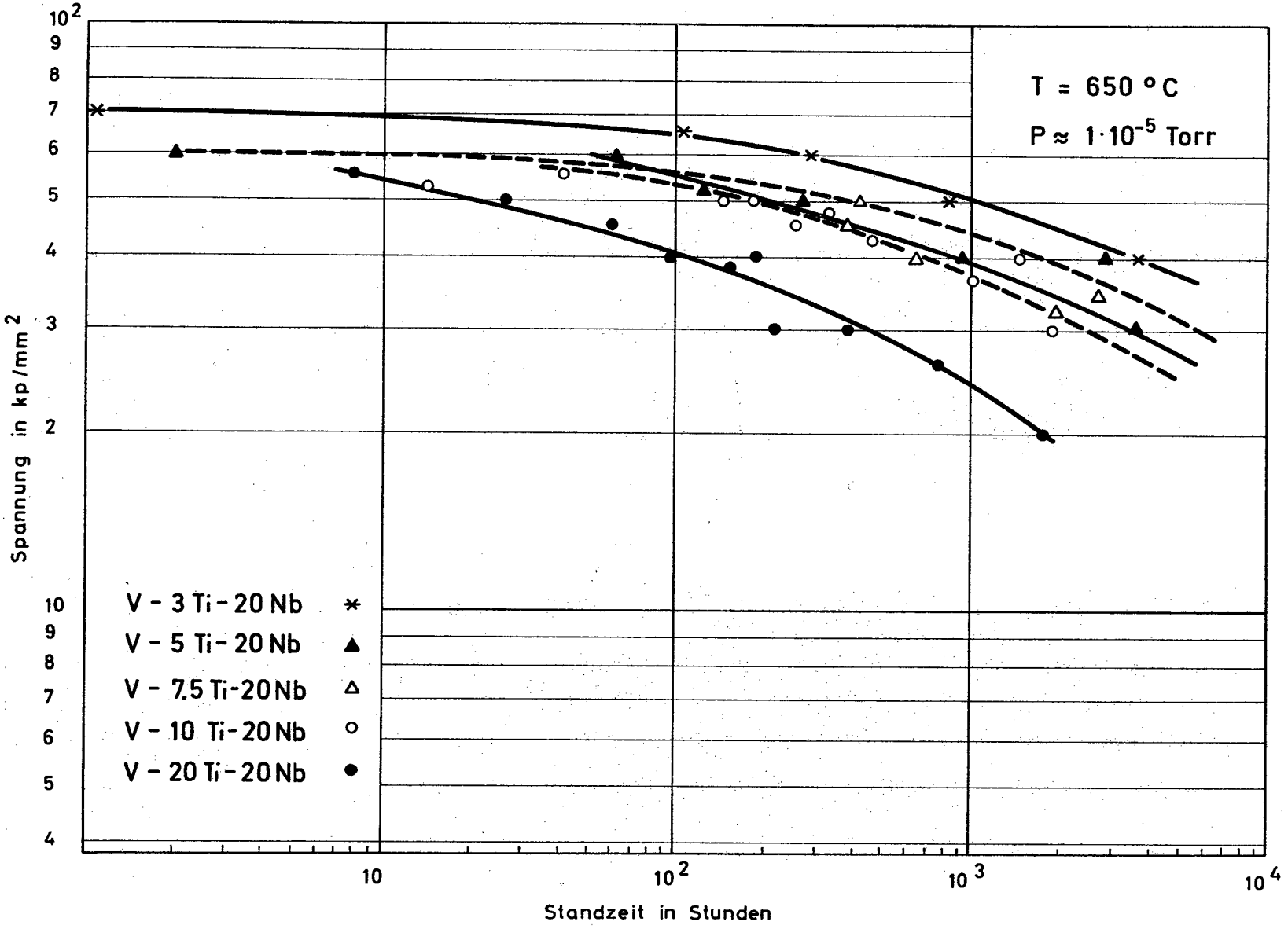

Bild 6: Einfluß des Ti-Gehaltes auf die Zeitstanfestigkeit von V-20 Nb-Legierungen

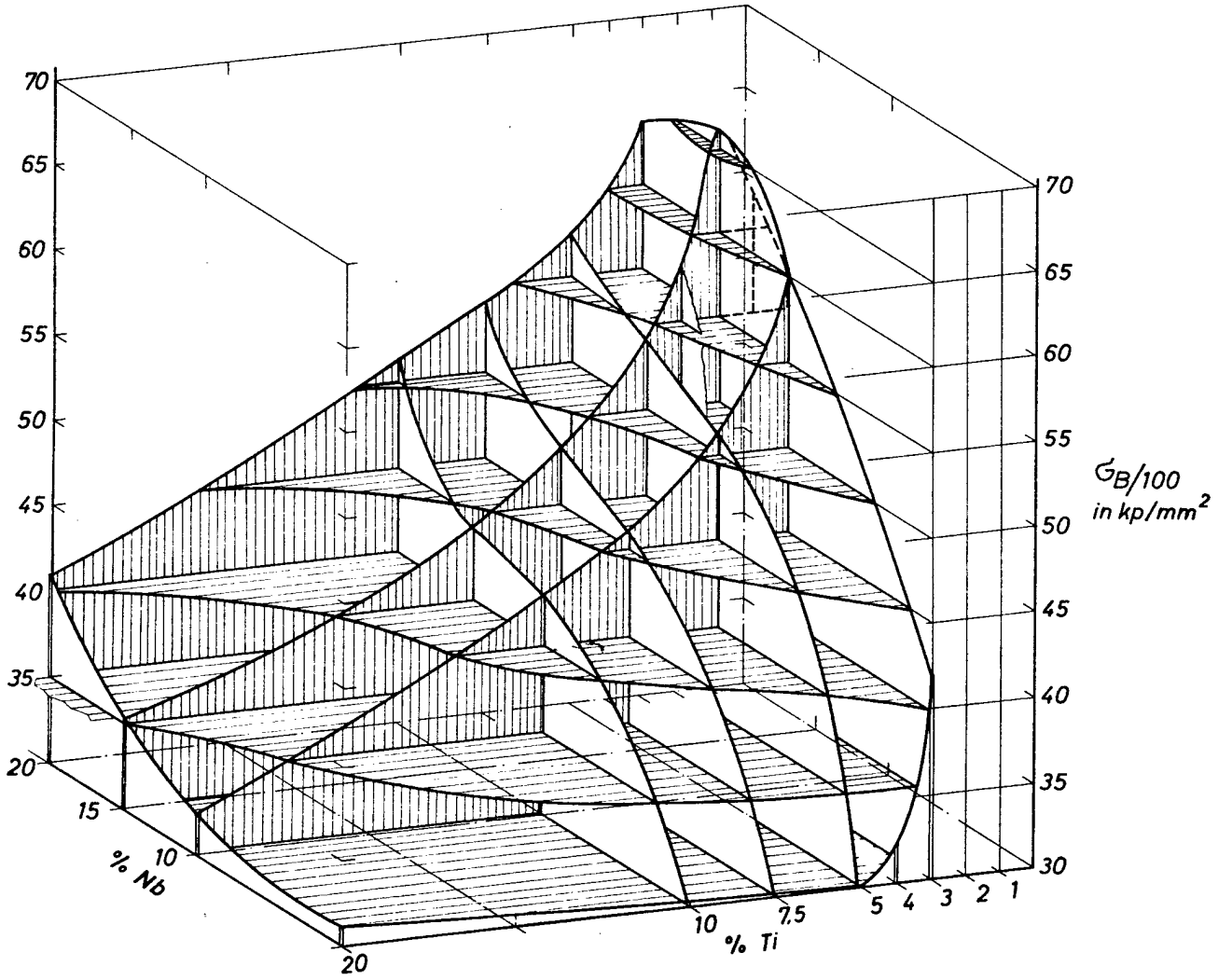

Bild 7 : 100-Stunden-Zeitstandfestigkeit von Vanadin-Basis-Legierungen in Abhängigkeit vom Titan- und Niob-Gehalt $T = 650°C$

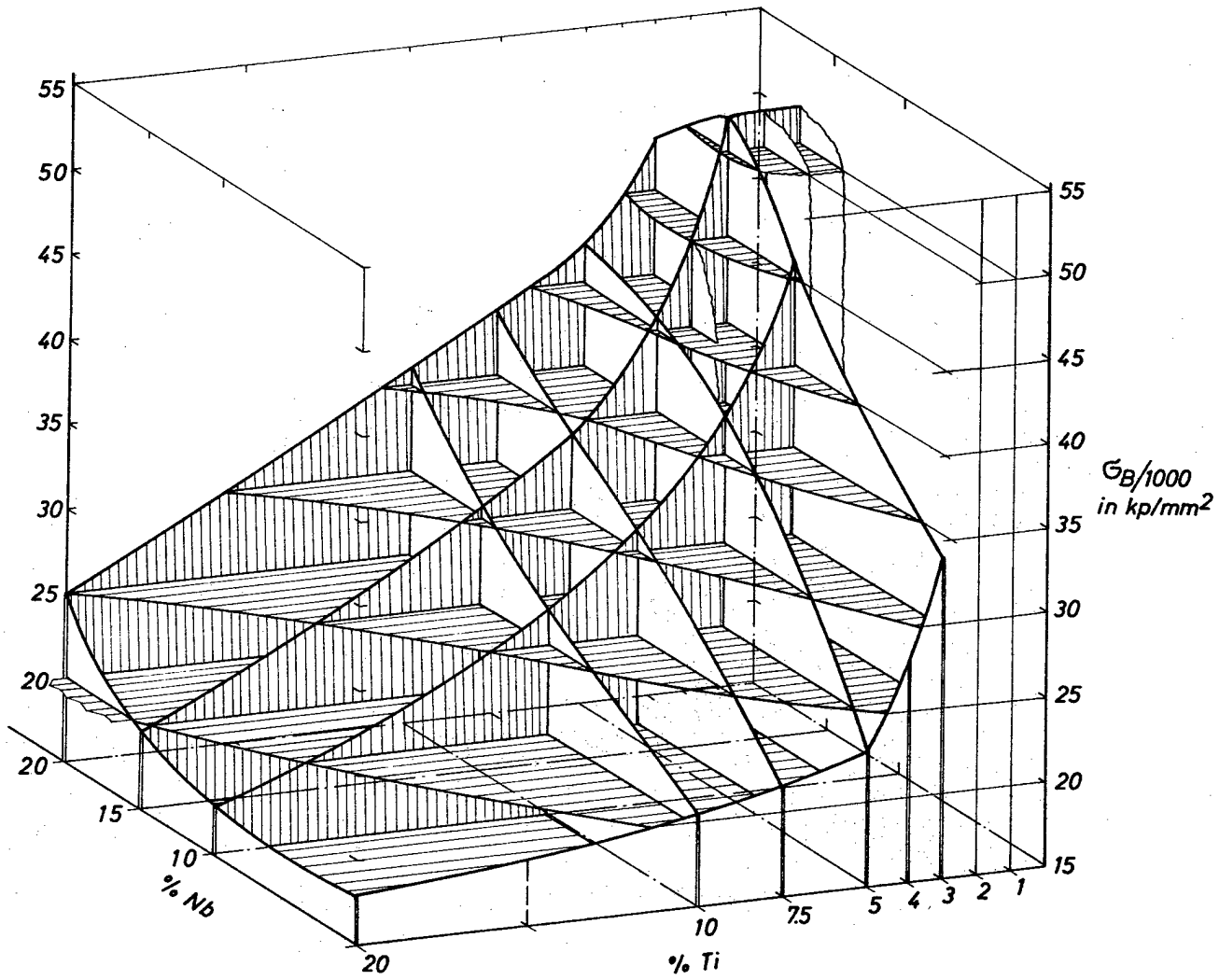

Bild 8 : 1000-Stunden-Zeitstandfestigkeit von Vanadin-Basis-Legierungen in Abhängigkeit vom Titan- und Niob-Gehalt (T = 650° C)

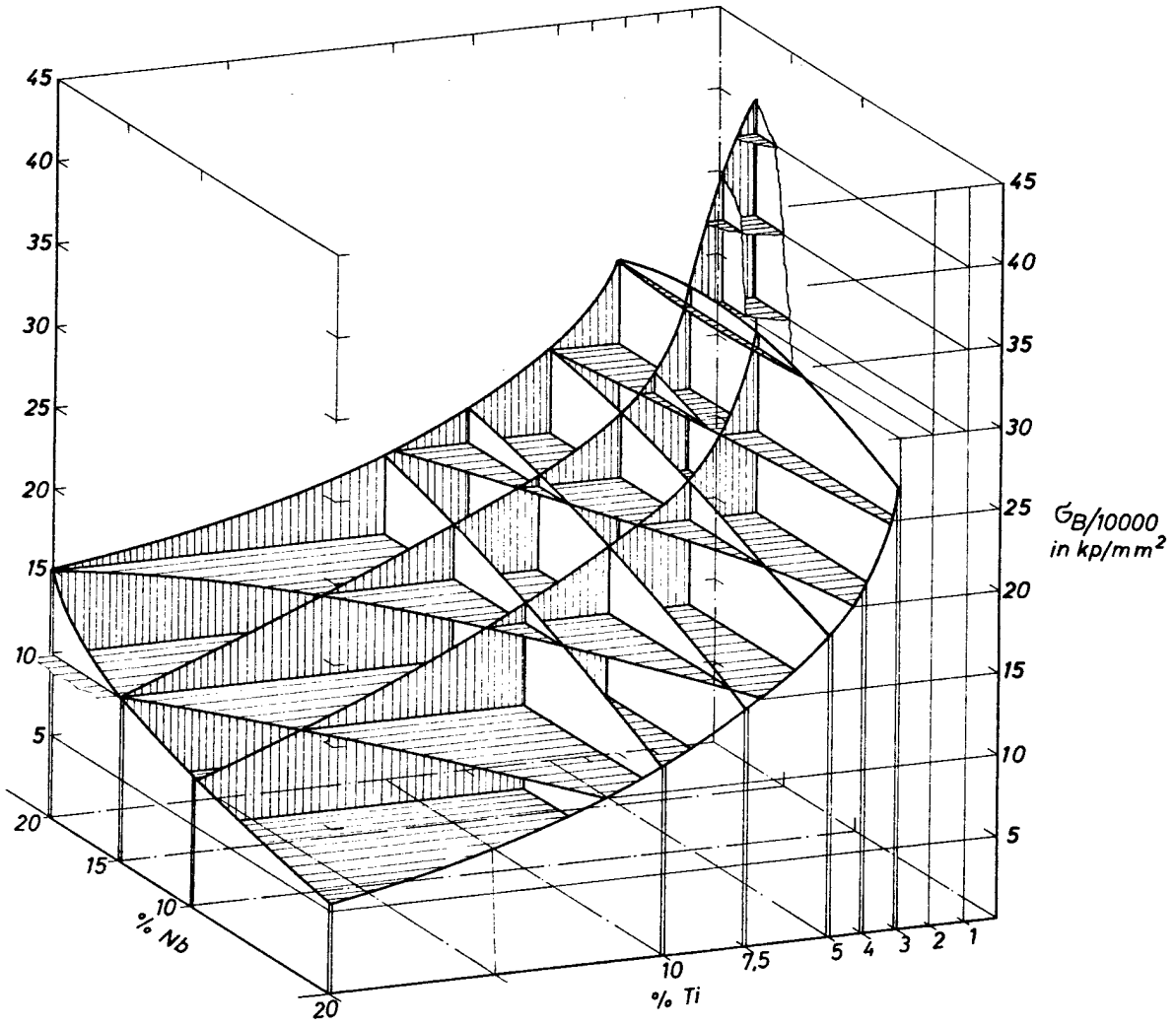

Bild 9 : 10000-Stunden-Zeitstandfestigkeit von Vanadin-Basis-Legierungen in Abhängigkeit vom Titan- und Niob-Gehalt (T= 650°C)

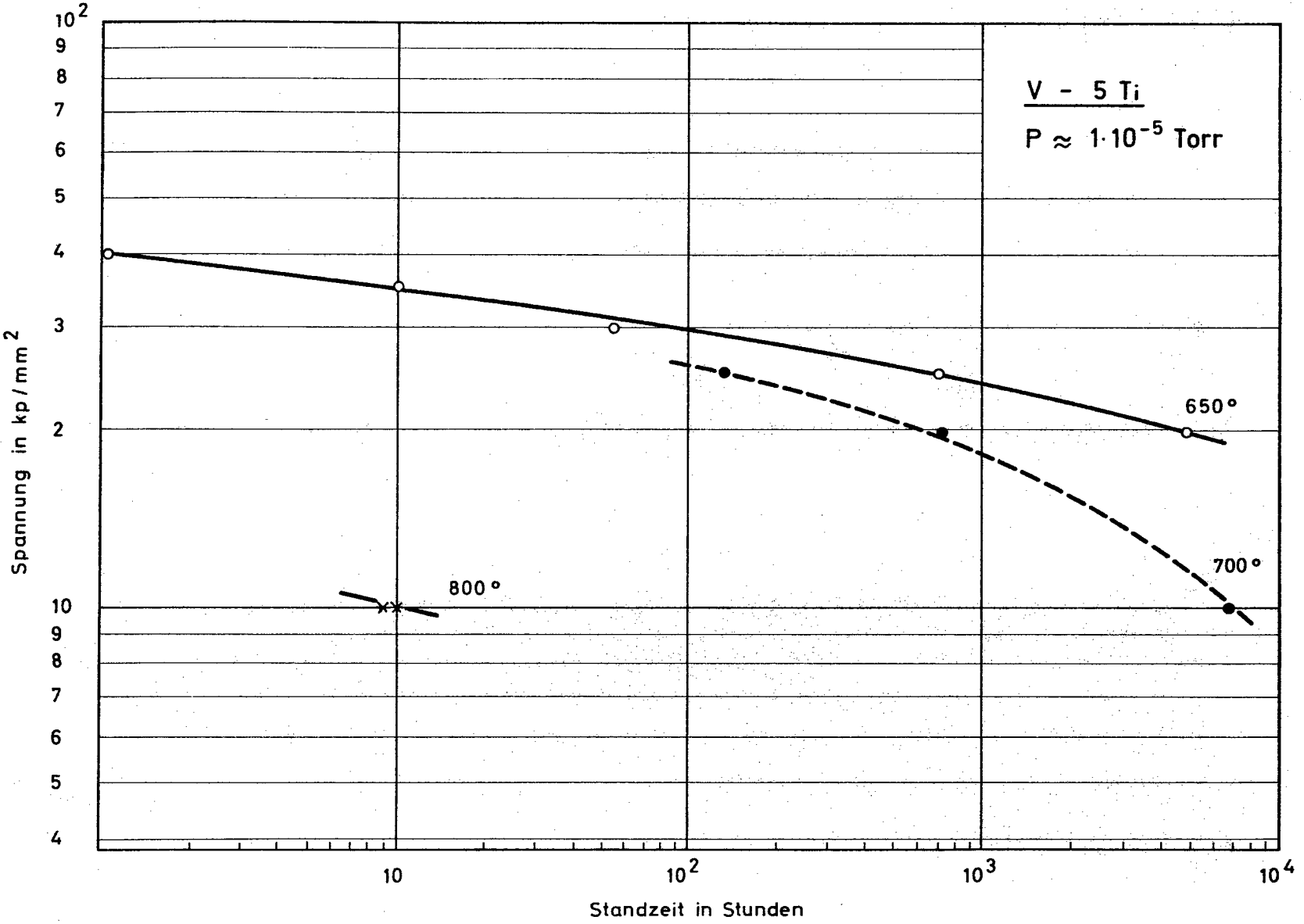

Bild *10* : Einfluß der Prüftemperatur auf die Zeitstandfestigkeit von V-5 Ti

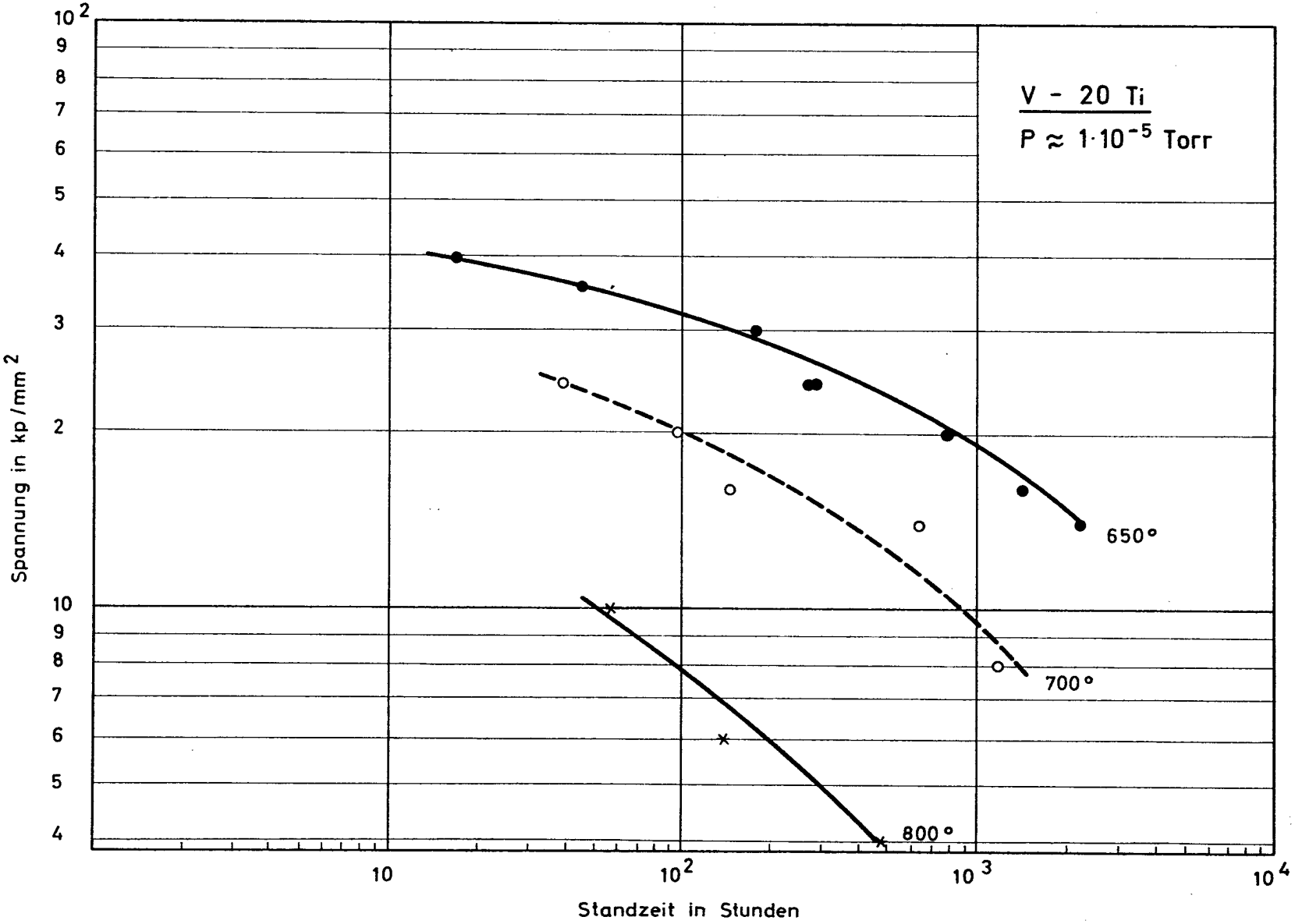

Bild 11: Einfluß der Prüftemperatur auf die Zeitstandfestigkeit von V - 20 Ti

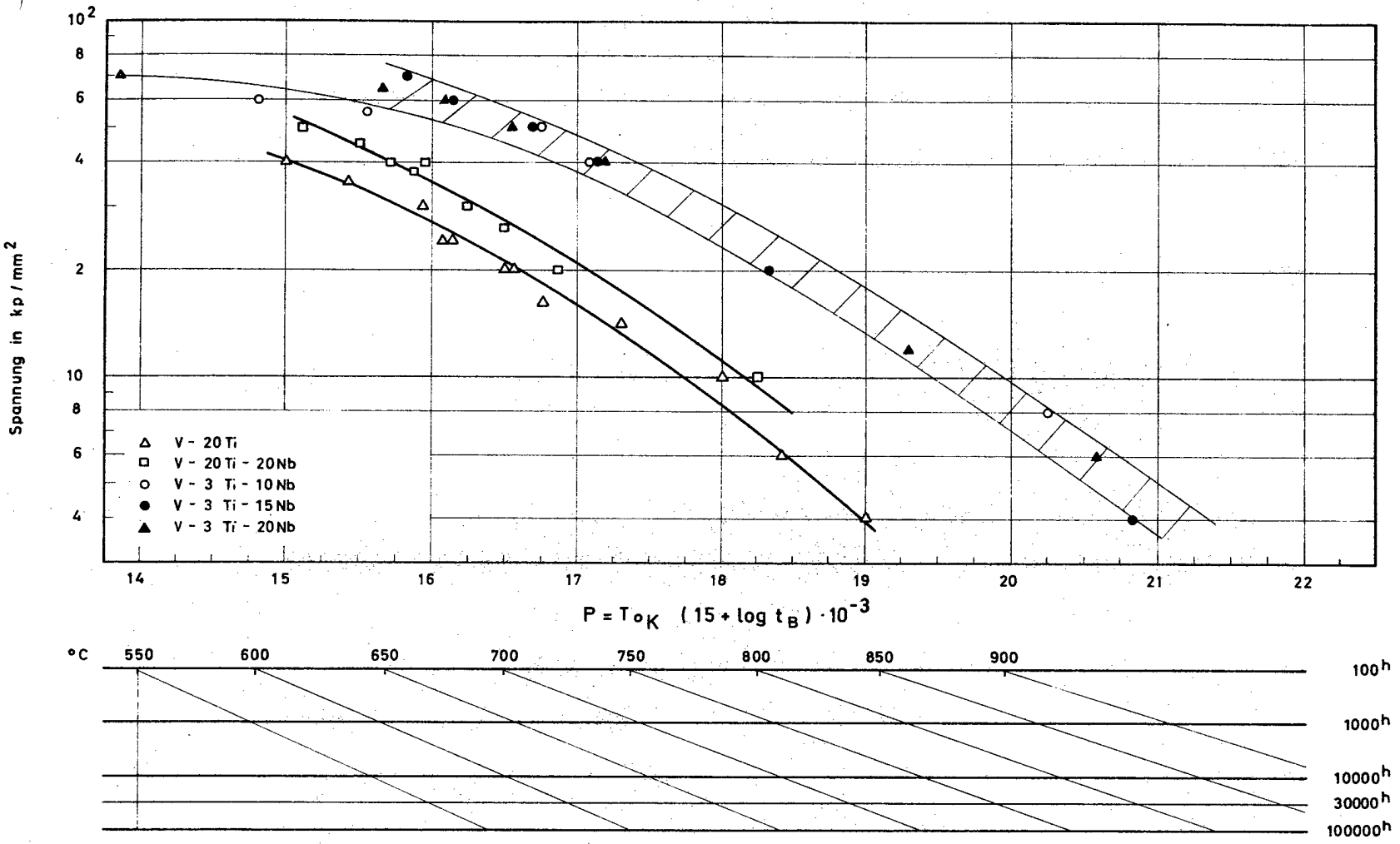

Bild 12 : Zeitstandfestigkeit in Abhängigkeit vom Larson - Miller - Parameter

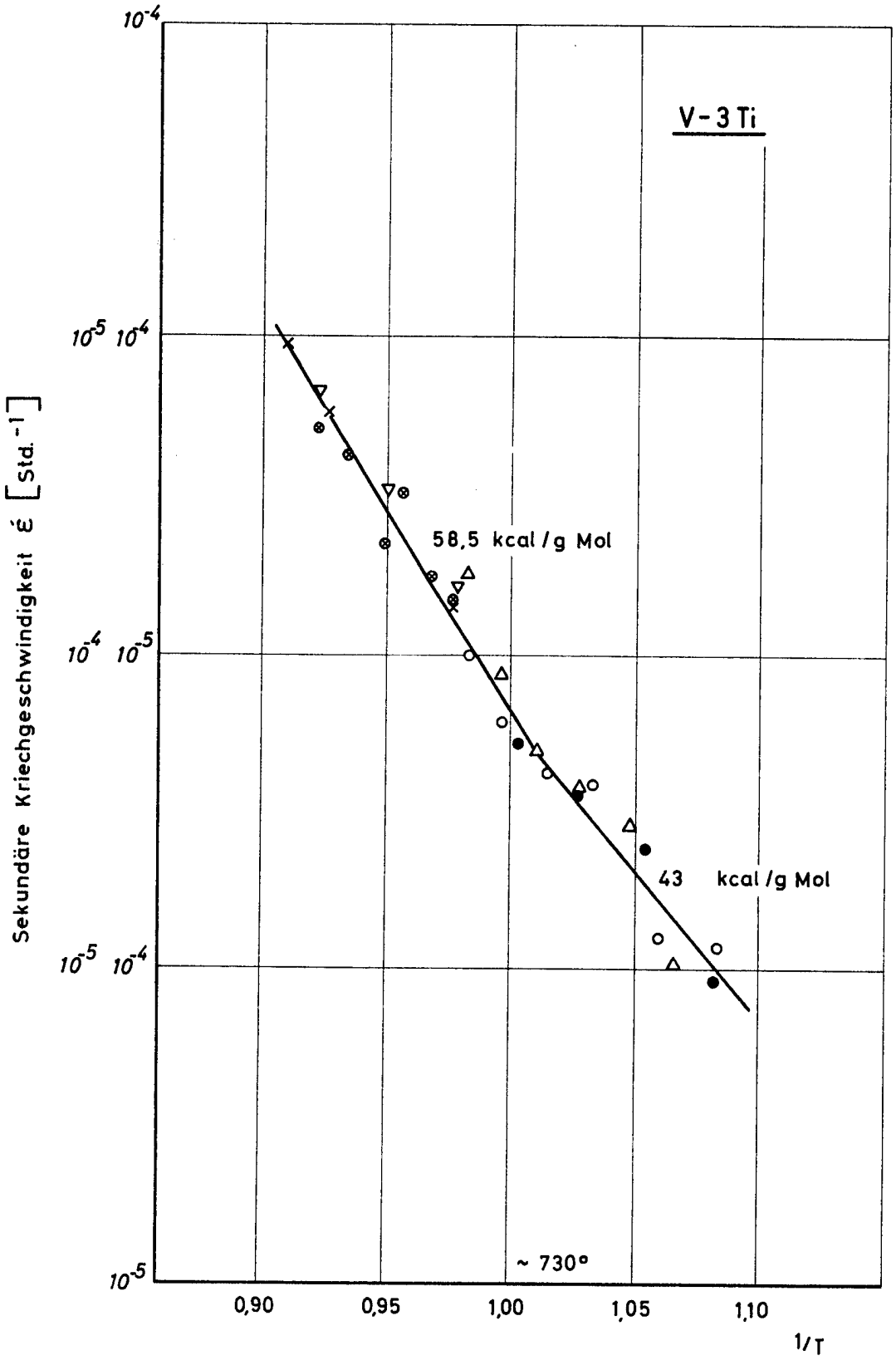

Bild *13* : Kriechgeschwindigkeit in Abhängigkeit von der Temperatur
(Vakuum≈$1 \cdot 10^{-5}$ Torr)

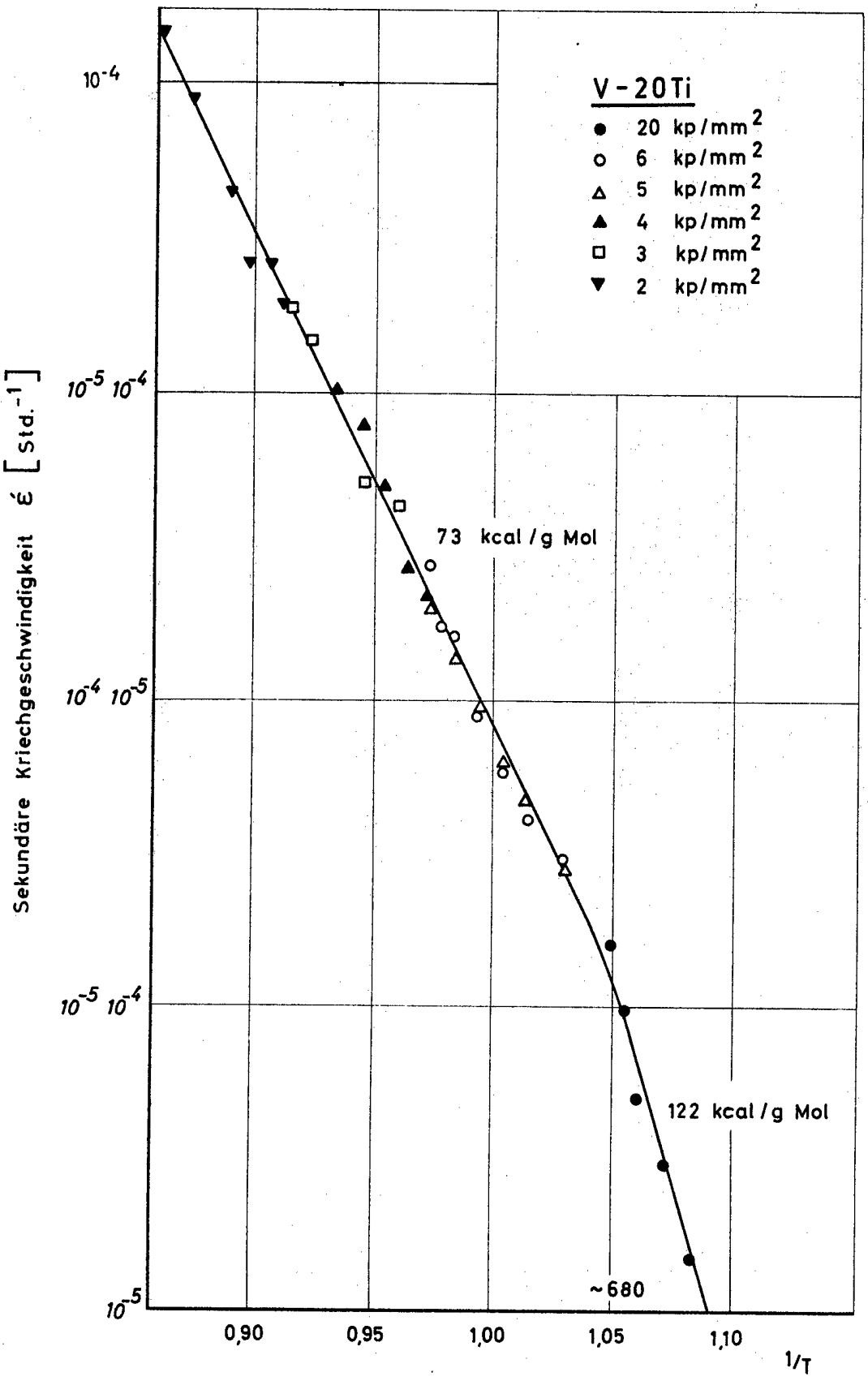

Bild 14 : Kriechgeschwindigkeit in Abhängigkeit von der Temperatur
(Vakuum ≈ $1 \cdot 10^{-5}$ Torr)

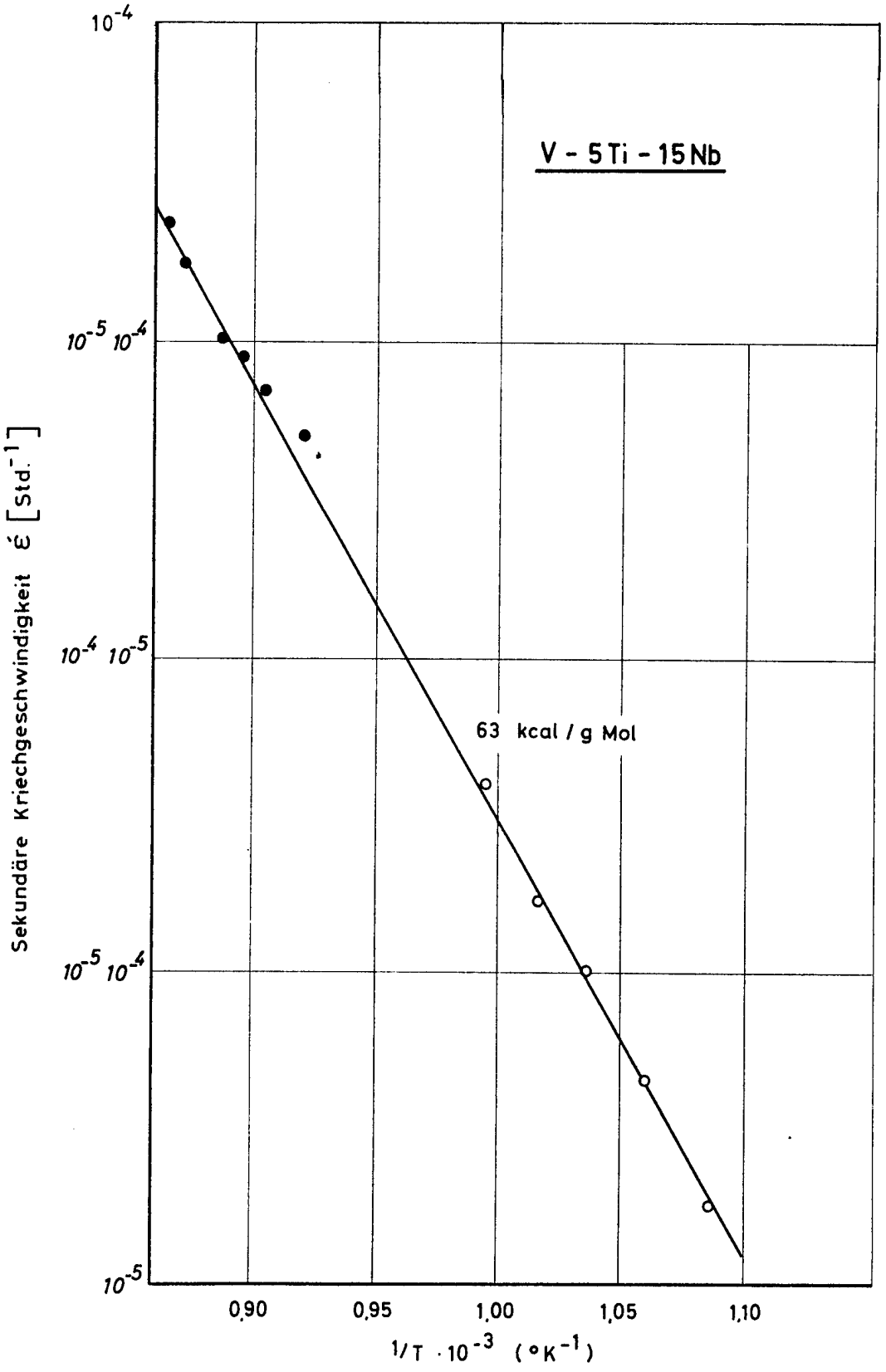

Bild 15 : Kriechgeschwindigkeit in Abhängigkeit von der Temperatur
(Vakuum ≈ $1 \cdot 10^{-5}$ Torr)

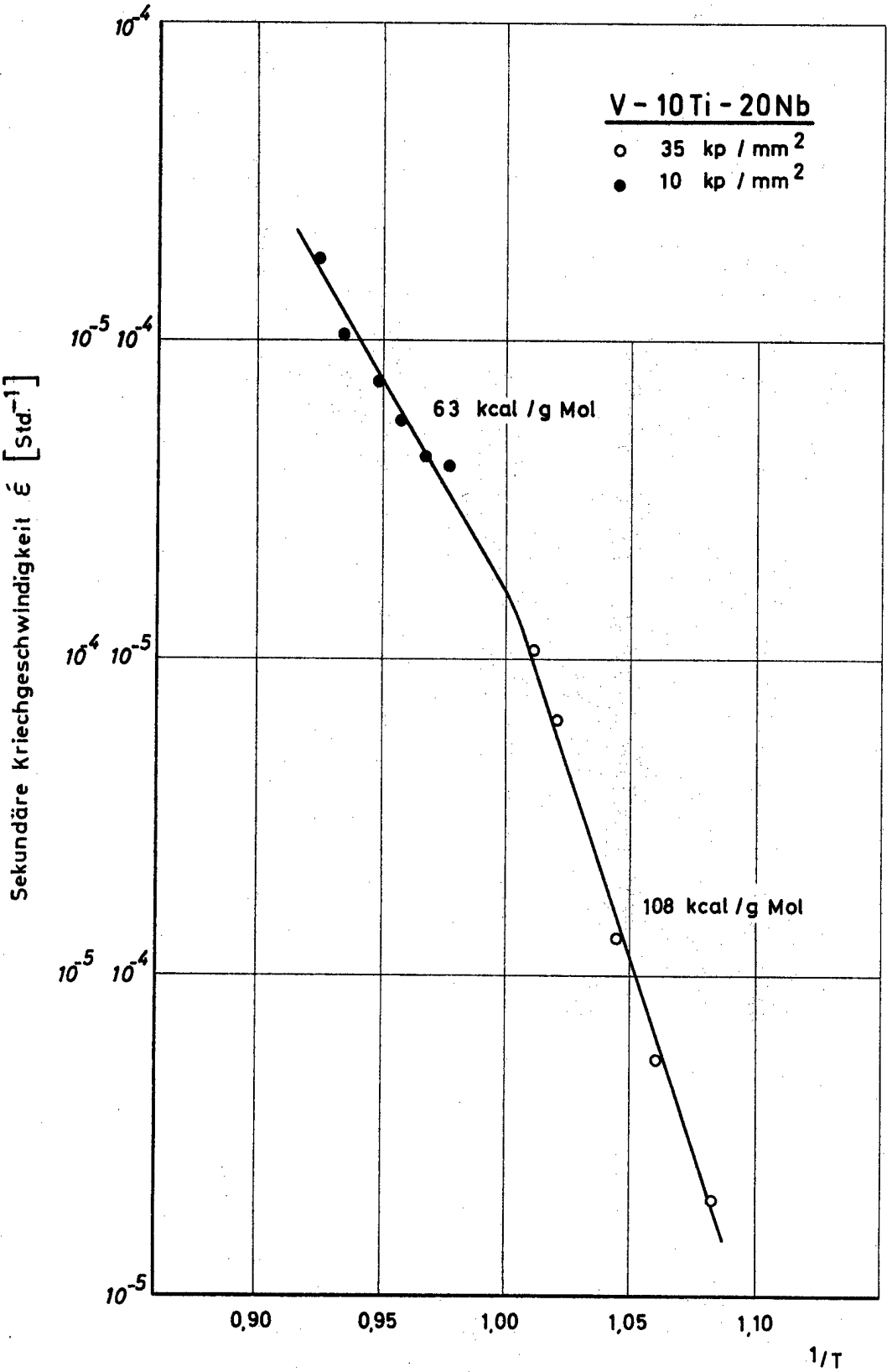

Bild 16: Kriechgeschwindigkeit in Abhängigkeit von der Temperatur
(Vakuum ≈ $1 \cdot 10^{-5}$ Torr)

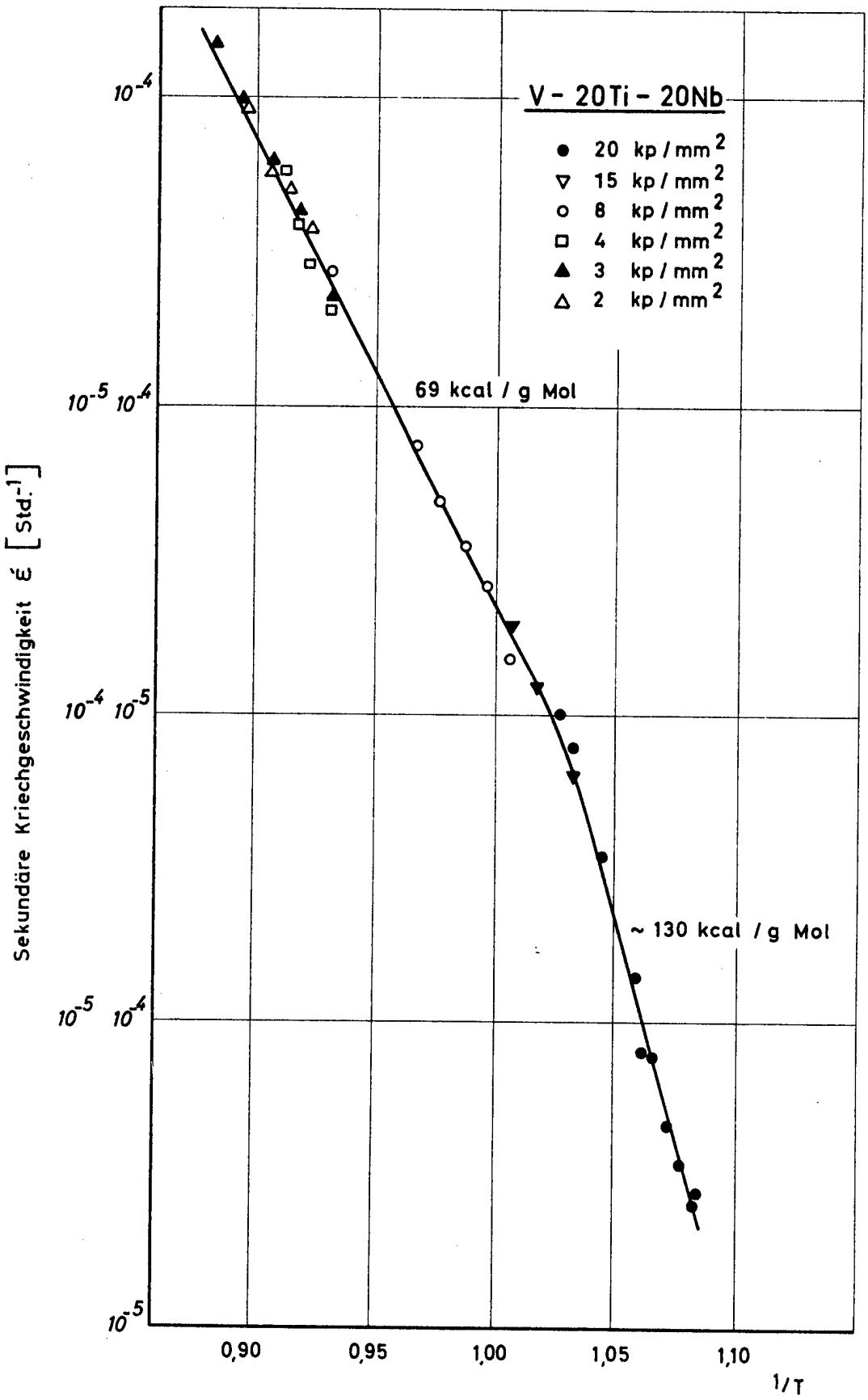

Bild 17 : Kriechgeschwindigkeit in Abhängigkeit von der Temperatur
(Vakuum ≈ $1 \cdot 10^{-5}$ Torr)

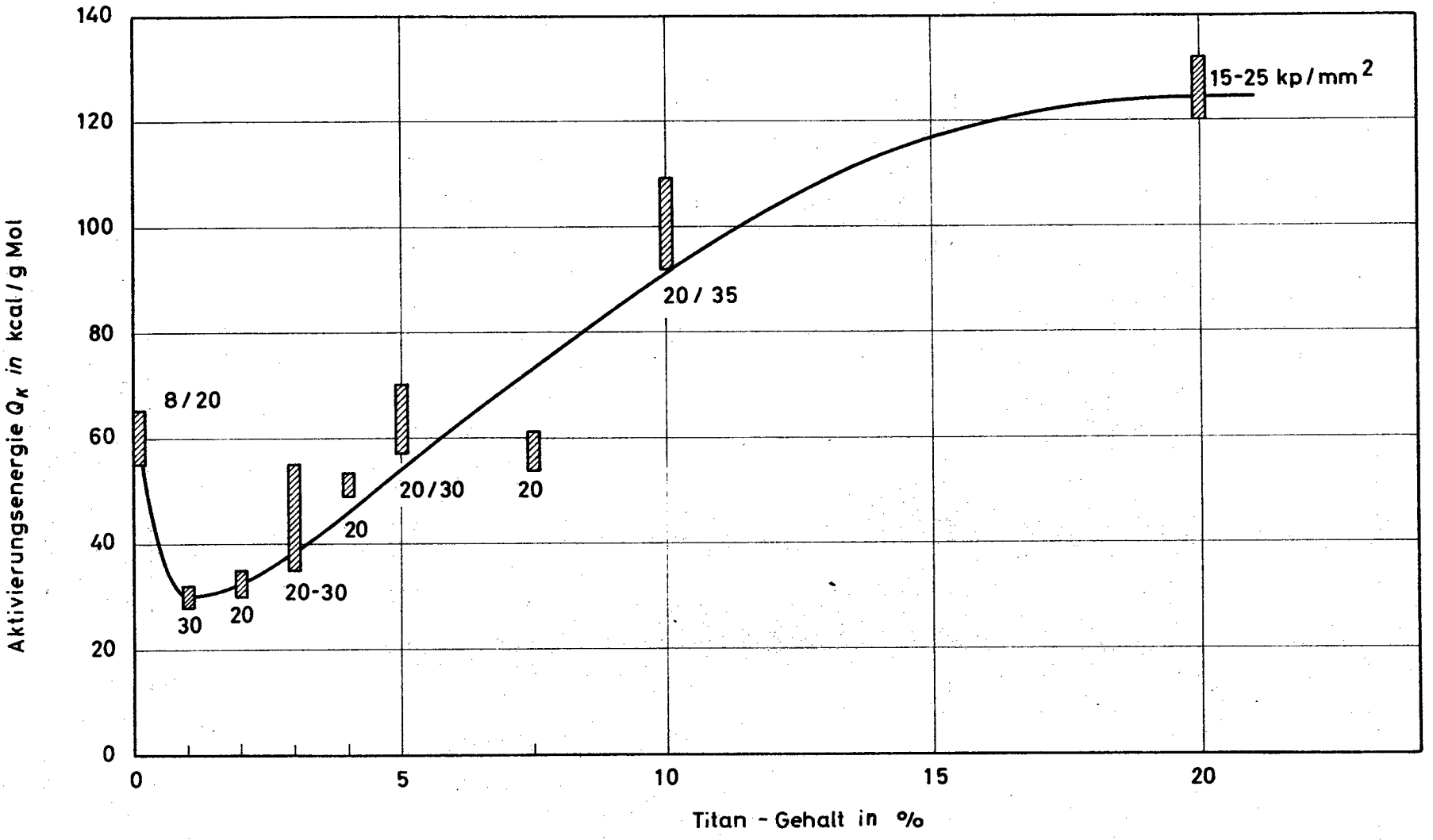

Bild 18 : Einfluß des Titan - Gehaltes auf die Aktivierungsenergie des Kriechens binärer und ternärer V - Legierungen (Temp. - Bereich 650 - 700 °C)

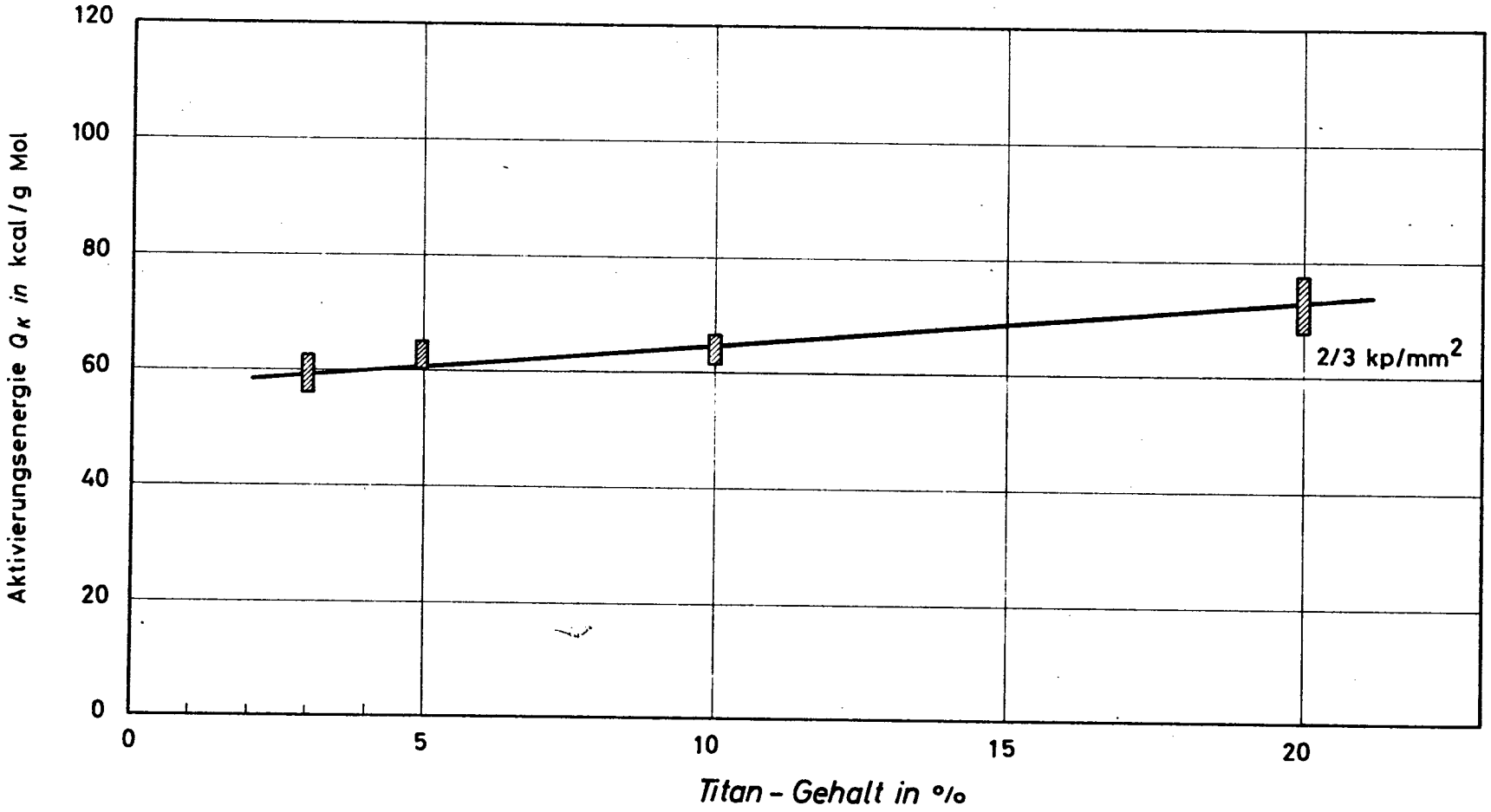

Bild 19: Einfluß des Titan - Gehaltes auf die Aktivierungsenergie des Kriechens bei Temperaturen > 750 °

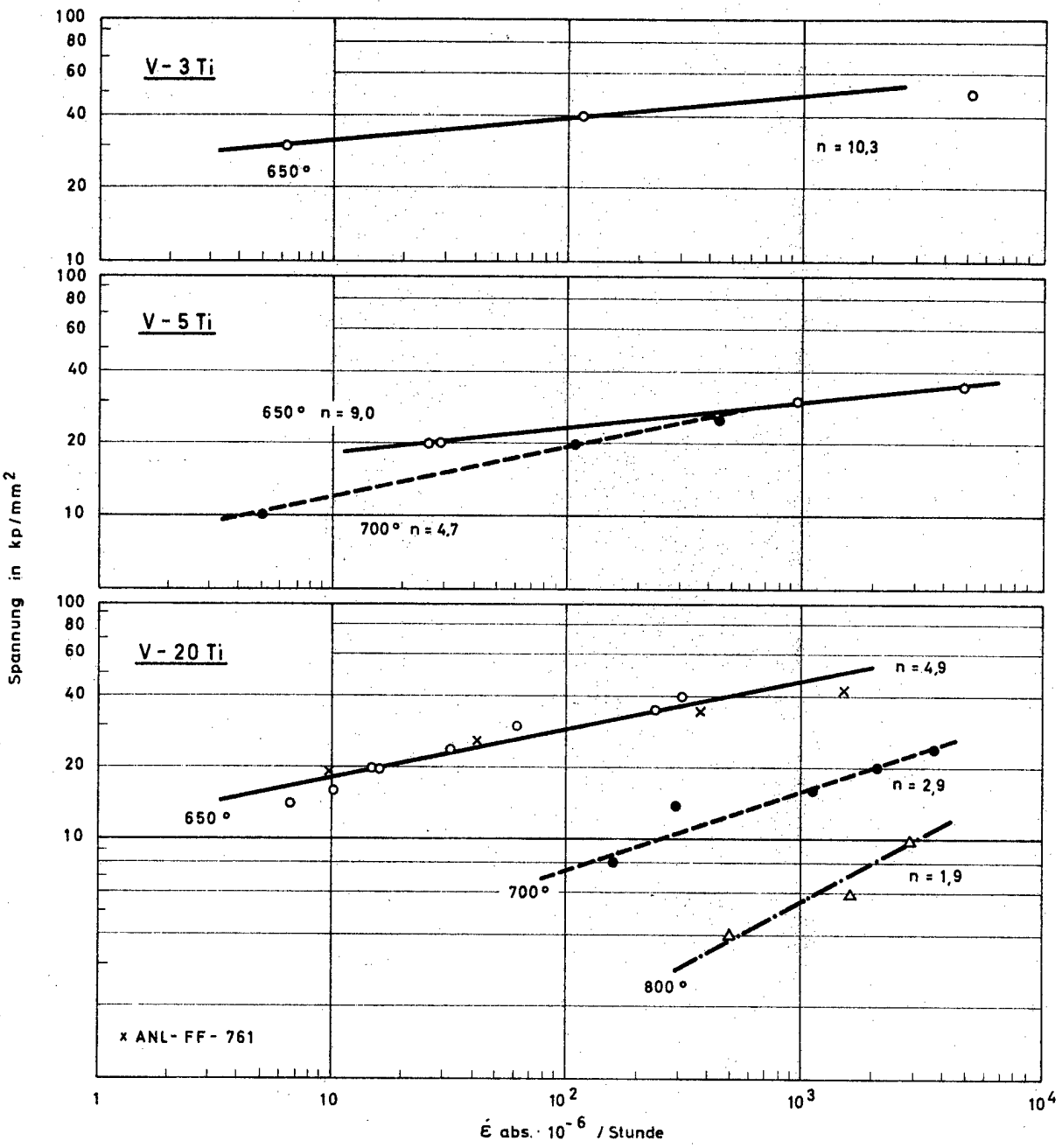

Bild *20*: Abhängigkeit der sekundären Kriechgeschwindigkeit von der Spannung ($P \approx 1 \cdot 10^{-5}$ Torr)

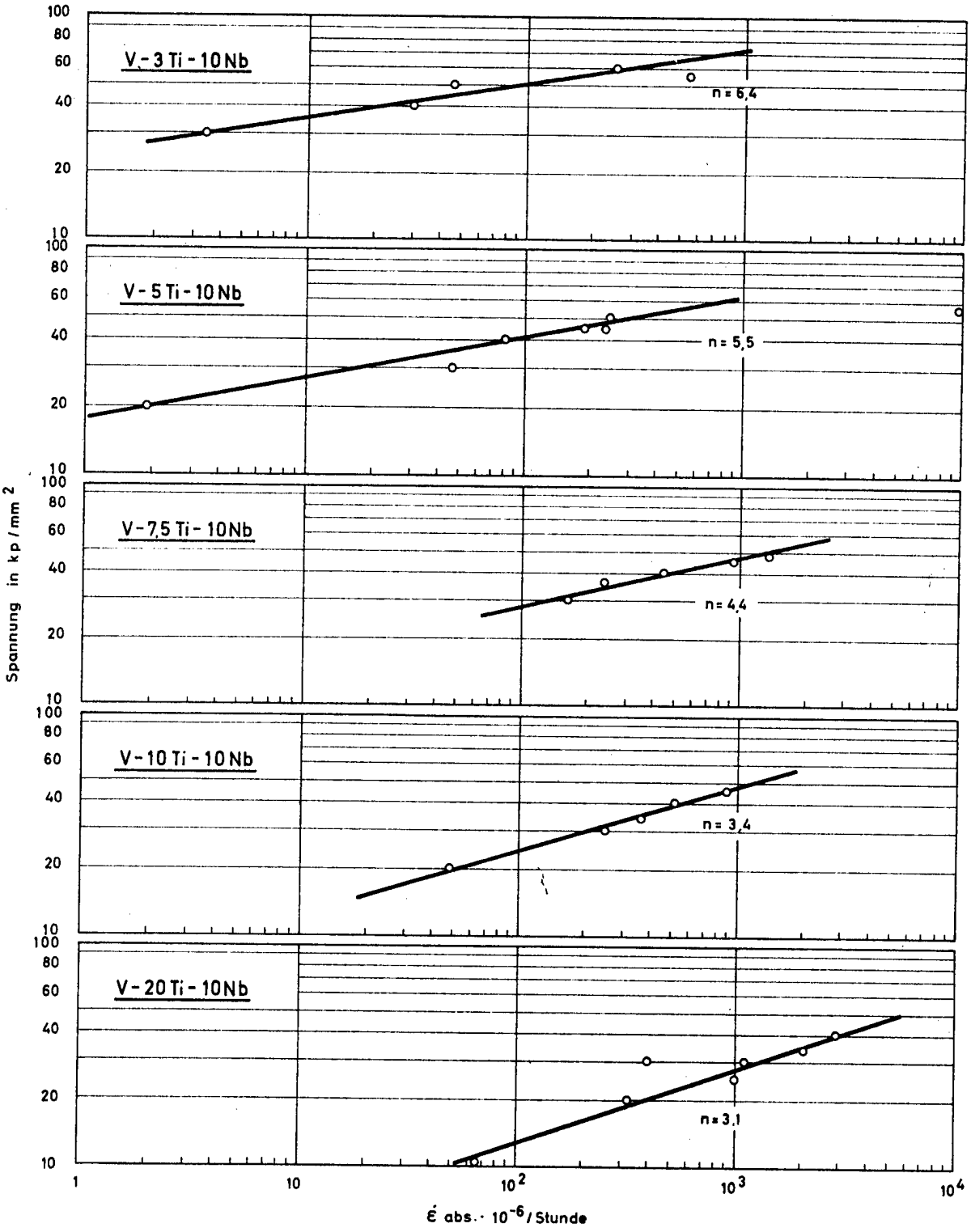

Bild 21 : Abhängigkeit der sekundären Kriechgeschwindigkeit von der Spannung bei 650°C
P≈ 1 · 10⁻⁵ Torr

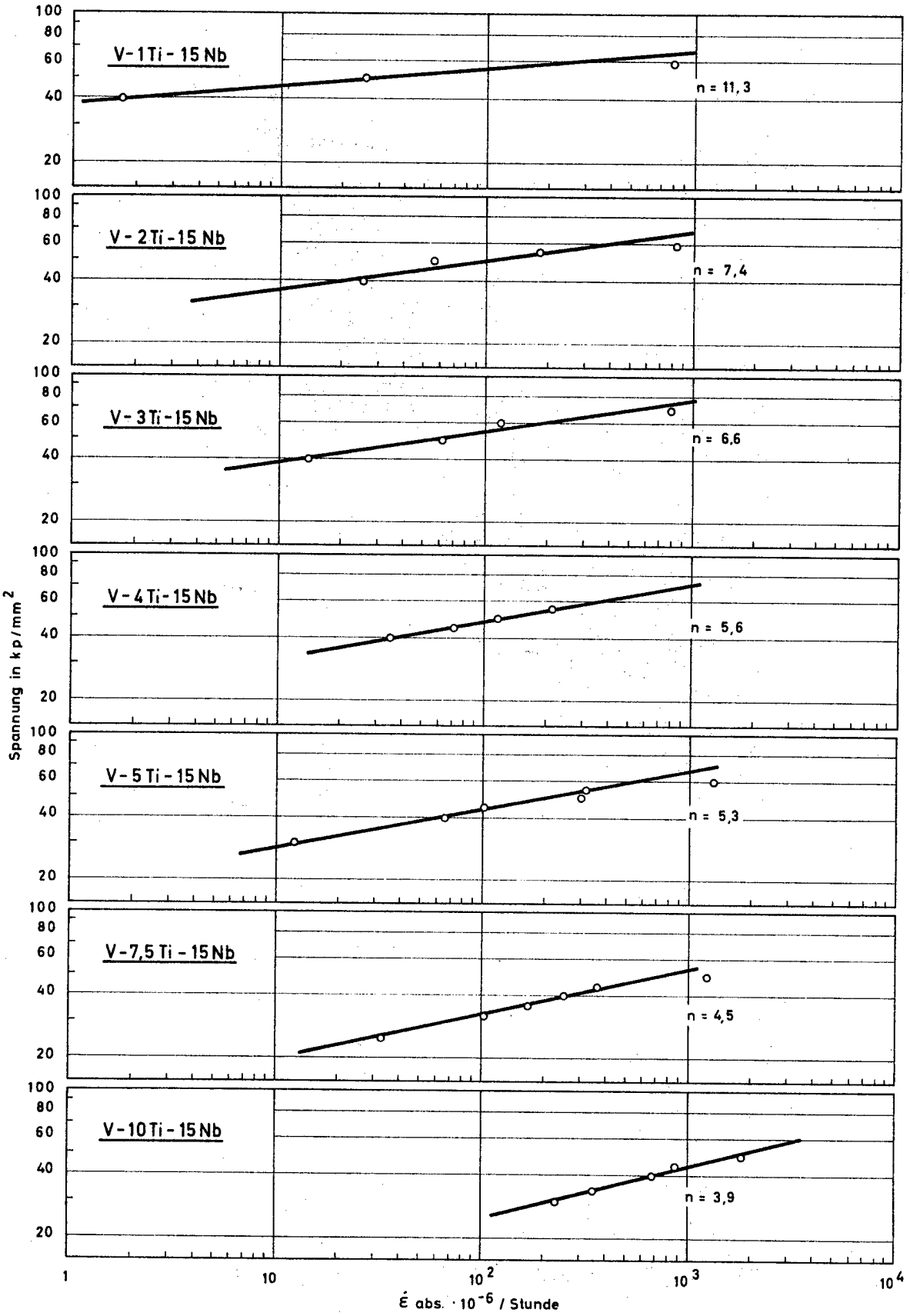

Bild 22 : Abhängigkeit der sekundären Kriechgeschwindigkeit von der Spannung bei 650°C
$P \approx 1 \cdot 10^{-5}$ Torr

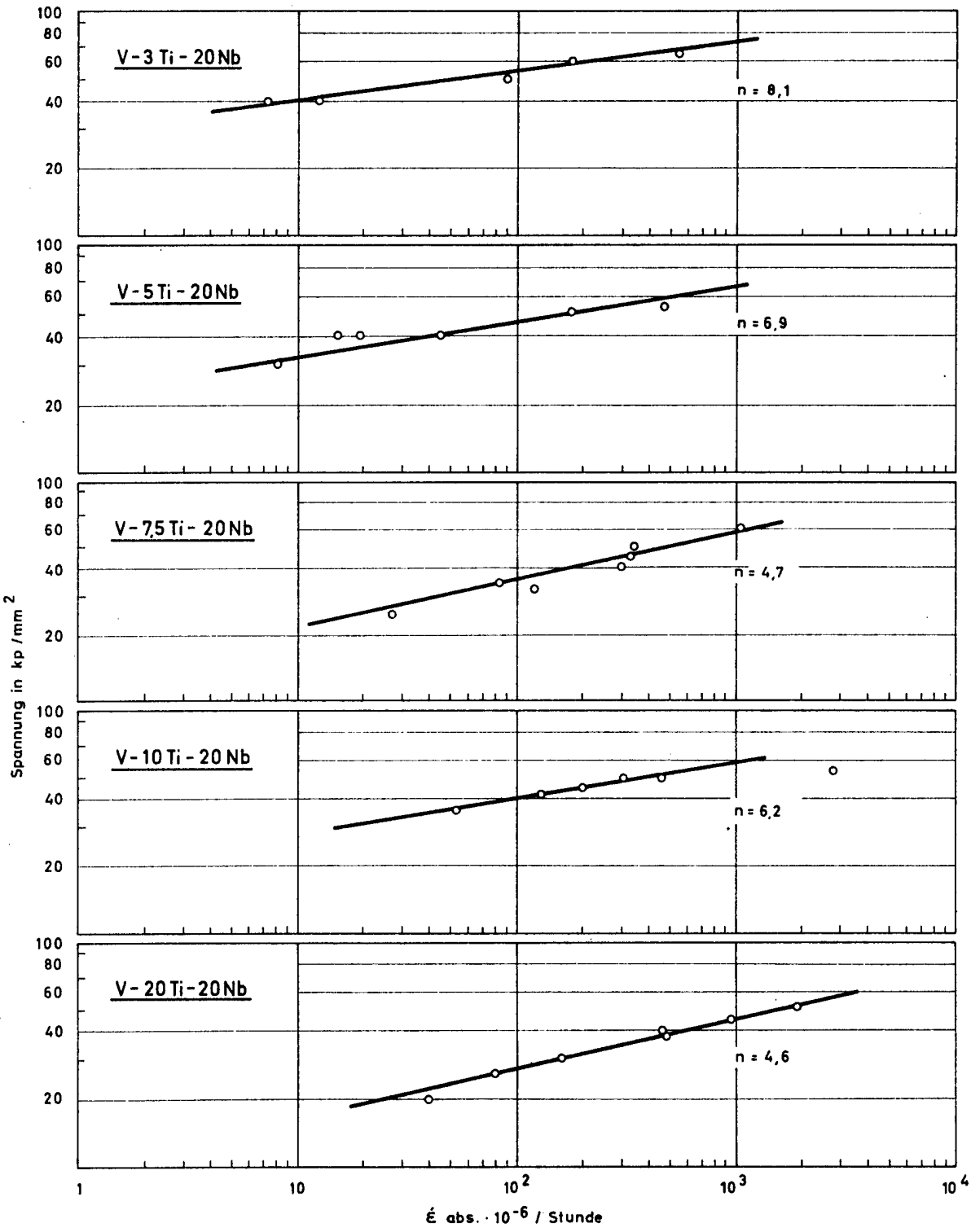

Bild 23 : Abhängigkeit der sekundären Kriechgeschwindigkeit von der Spannung bei 650 °C
$P \approx 1 \cdot 10^{-5}$ Torr

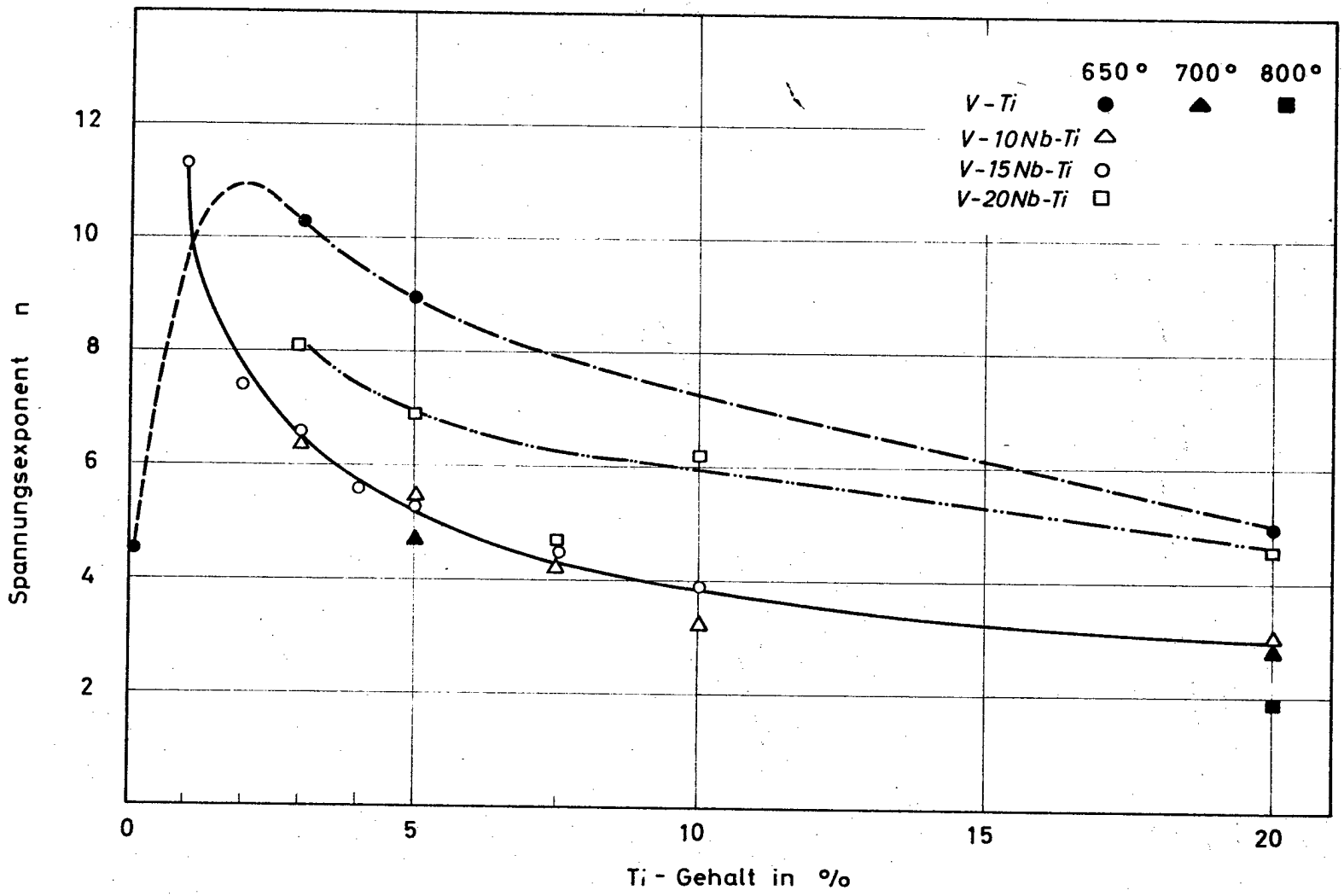

Bild 24: Einfluß des Ti - Gehaltes auf den Spannungsexponenten binärer und ternärer Vanadin - Legierungen

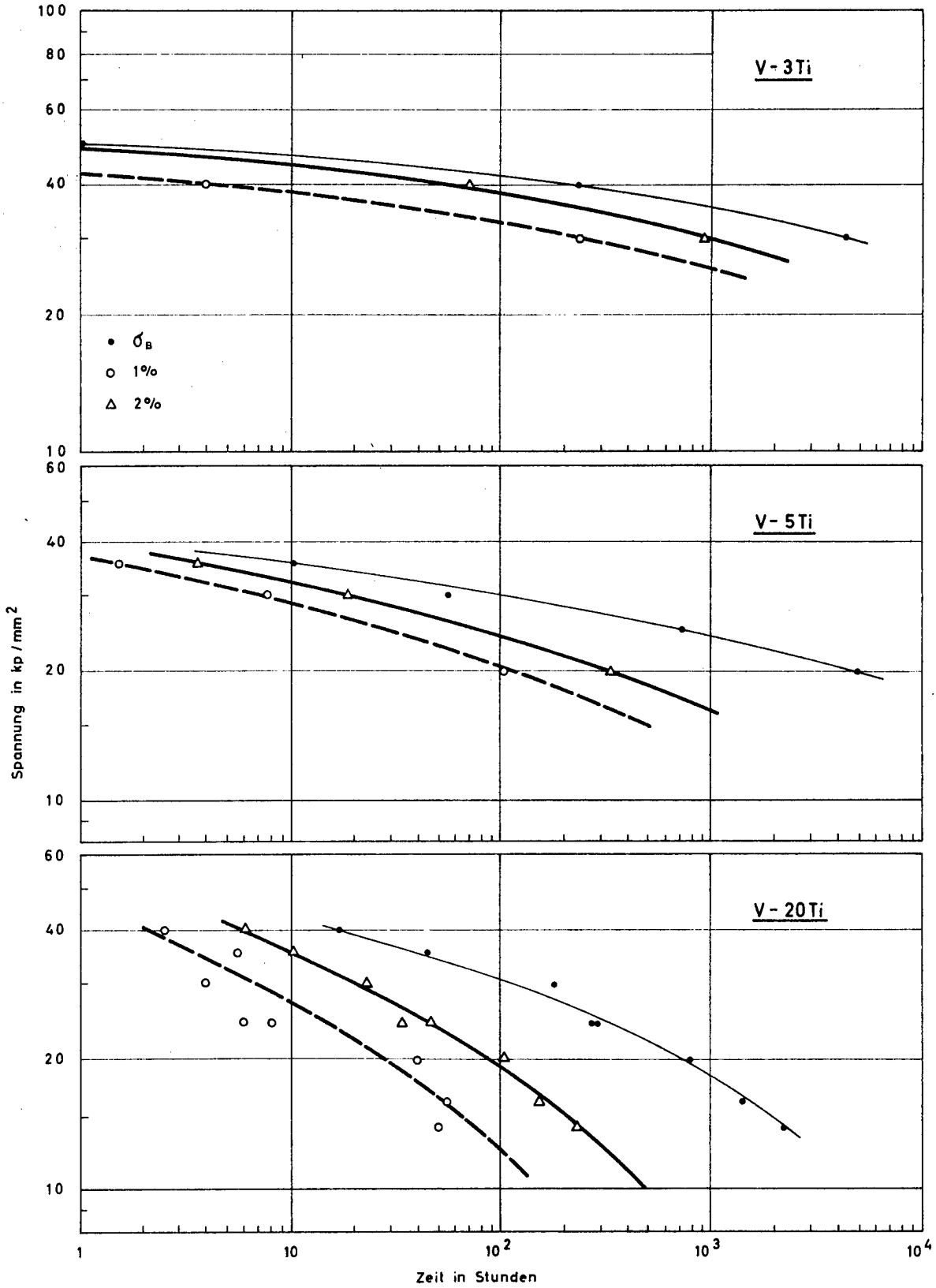

Bild 25 : Zeit - Dehngrenzen in Abhängigkeit von der Spannung T = 650 °C
$P \approx 1 \cdot 10^{-5}$ Torr

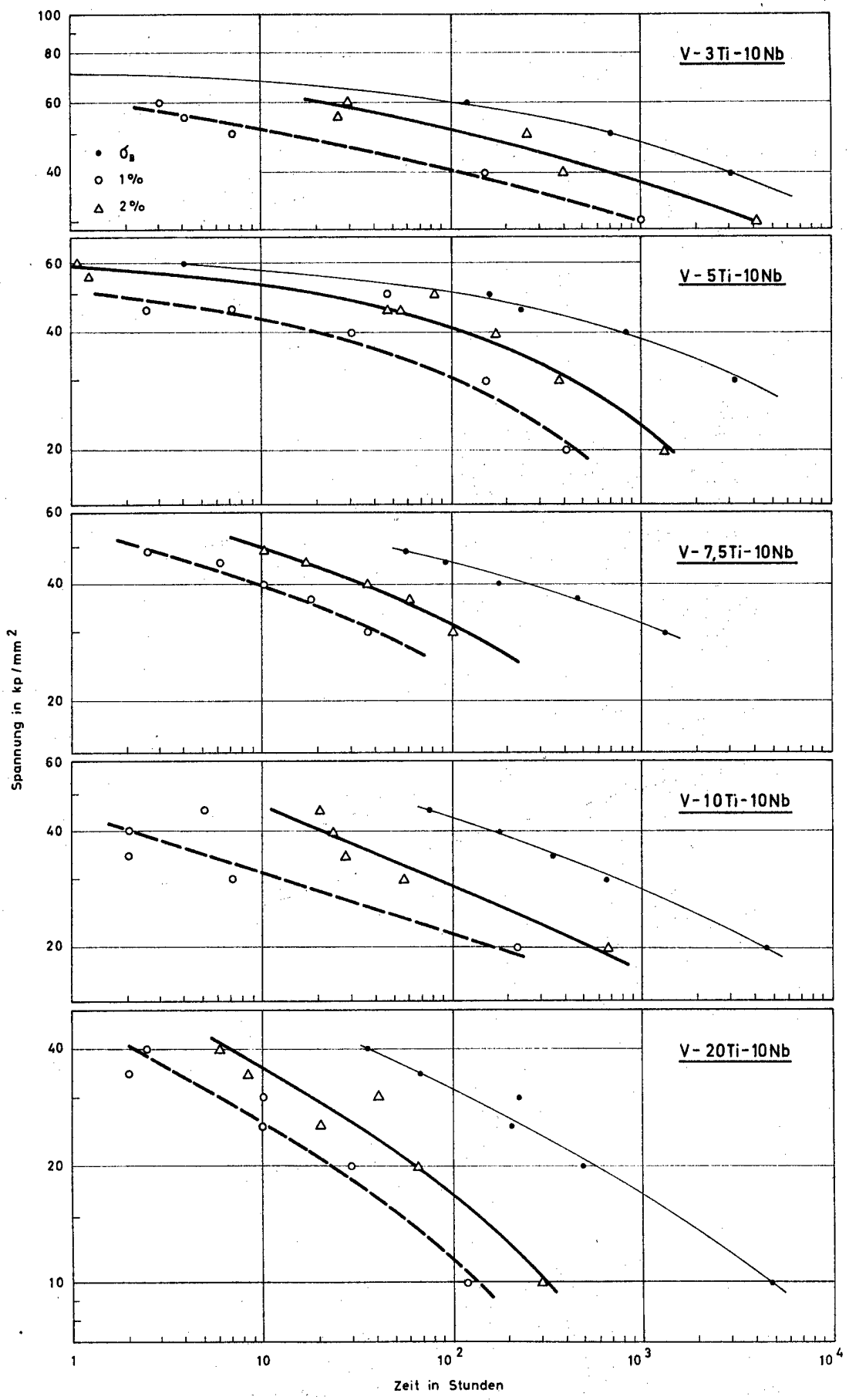

Bild 26 : Zeit - Dehngrenzen in Abhängigkeit von der Spannung T = 650 °C
P ≈ 1 · 10⁻⁵ Torr

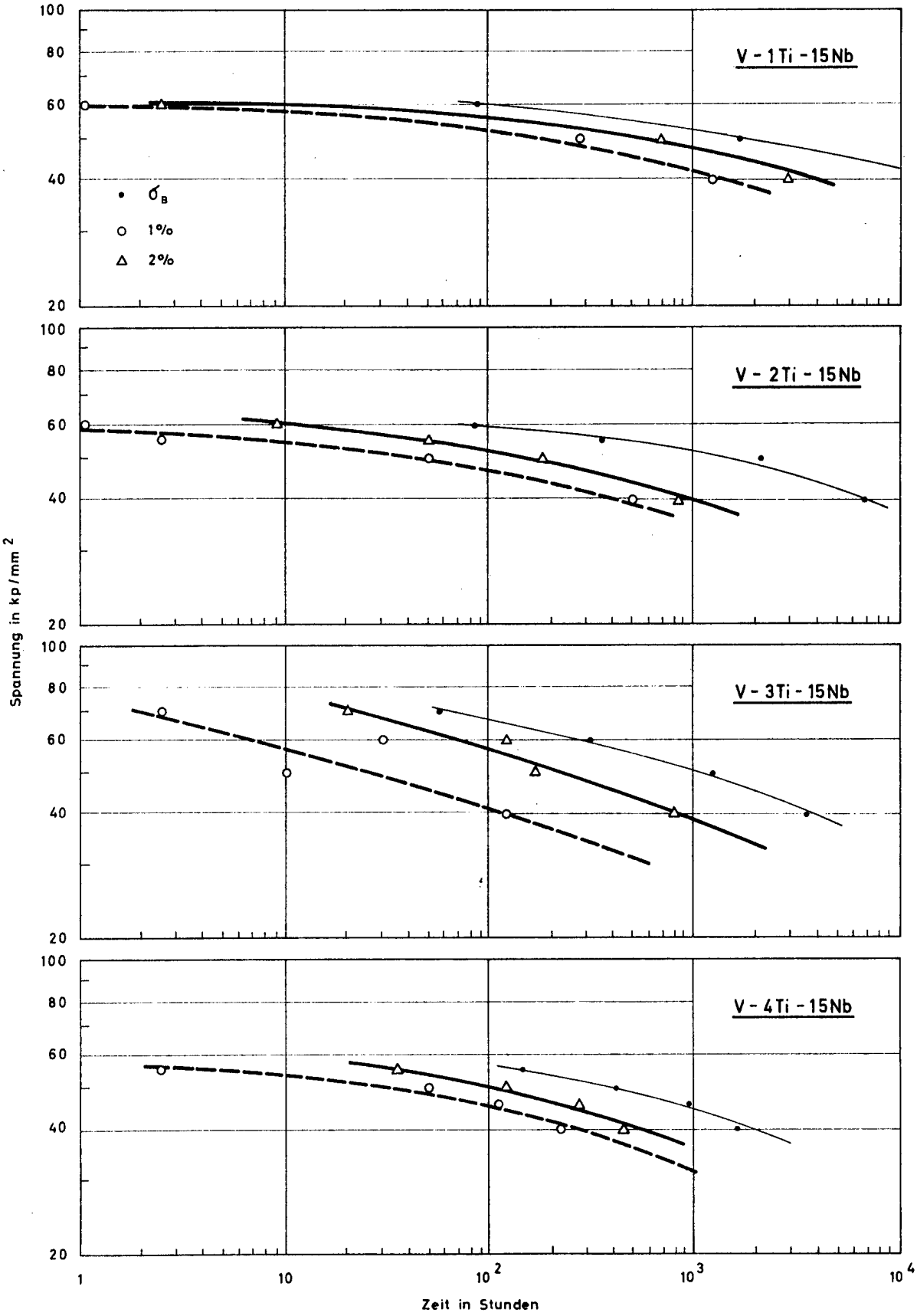

Bild 27: Zeit - Dehngrenzen in Abhängigkeit von der Spannung T = 650 °C
P ≈ 1 · 10⁻⁵ Torr

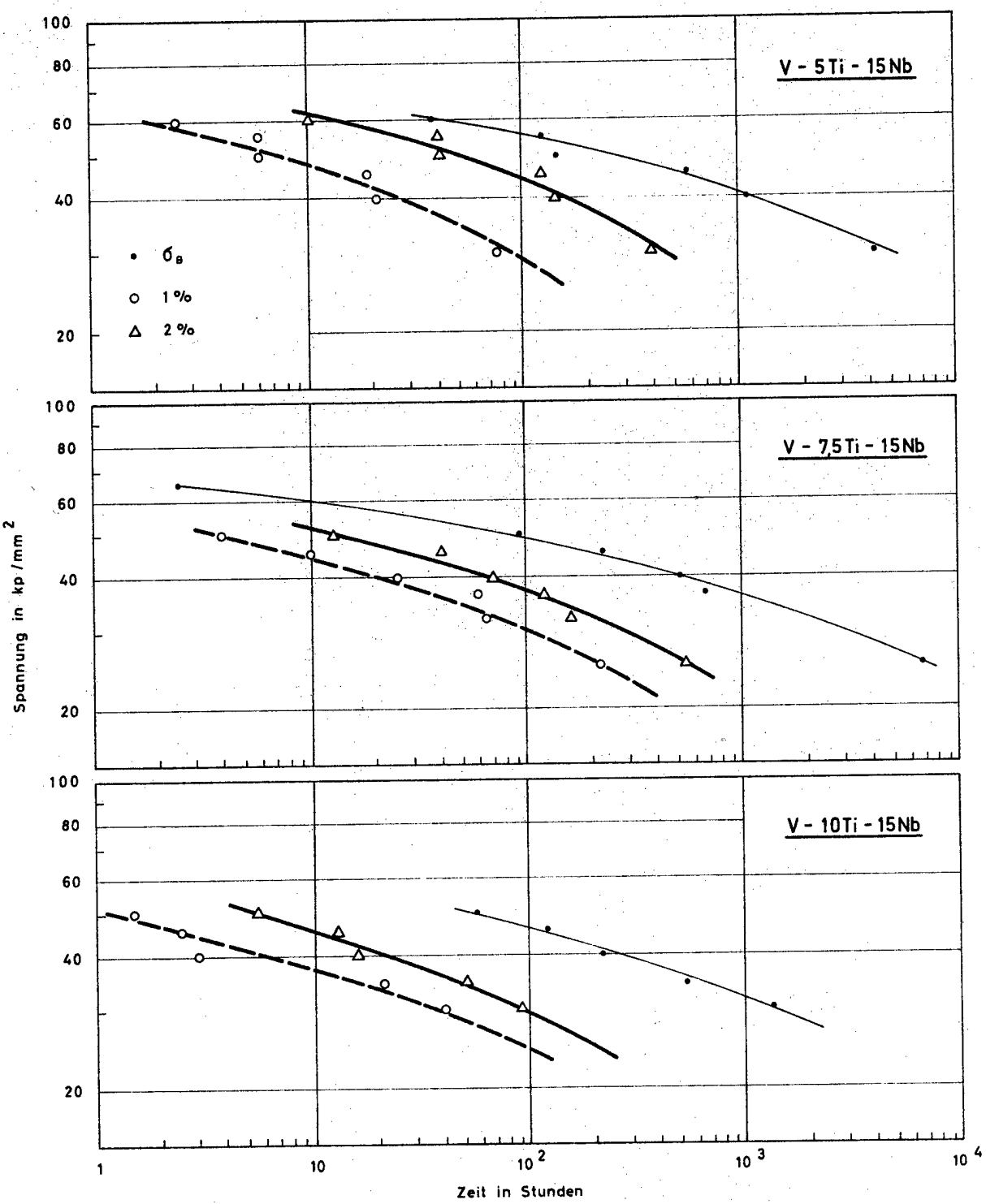

Bild 28 : Zeit - Dehngrenzen in Abhängigkeit von der Spannung T = 650 °C

$P \approx 1 \cdot 10^{-5}$ Torr

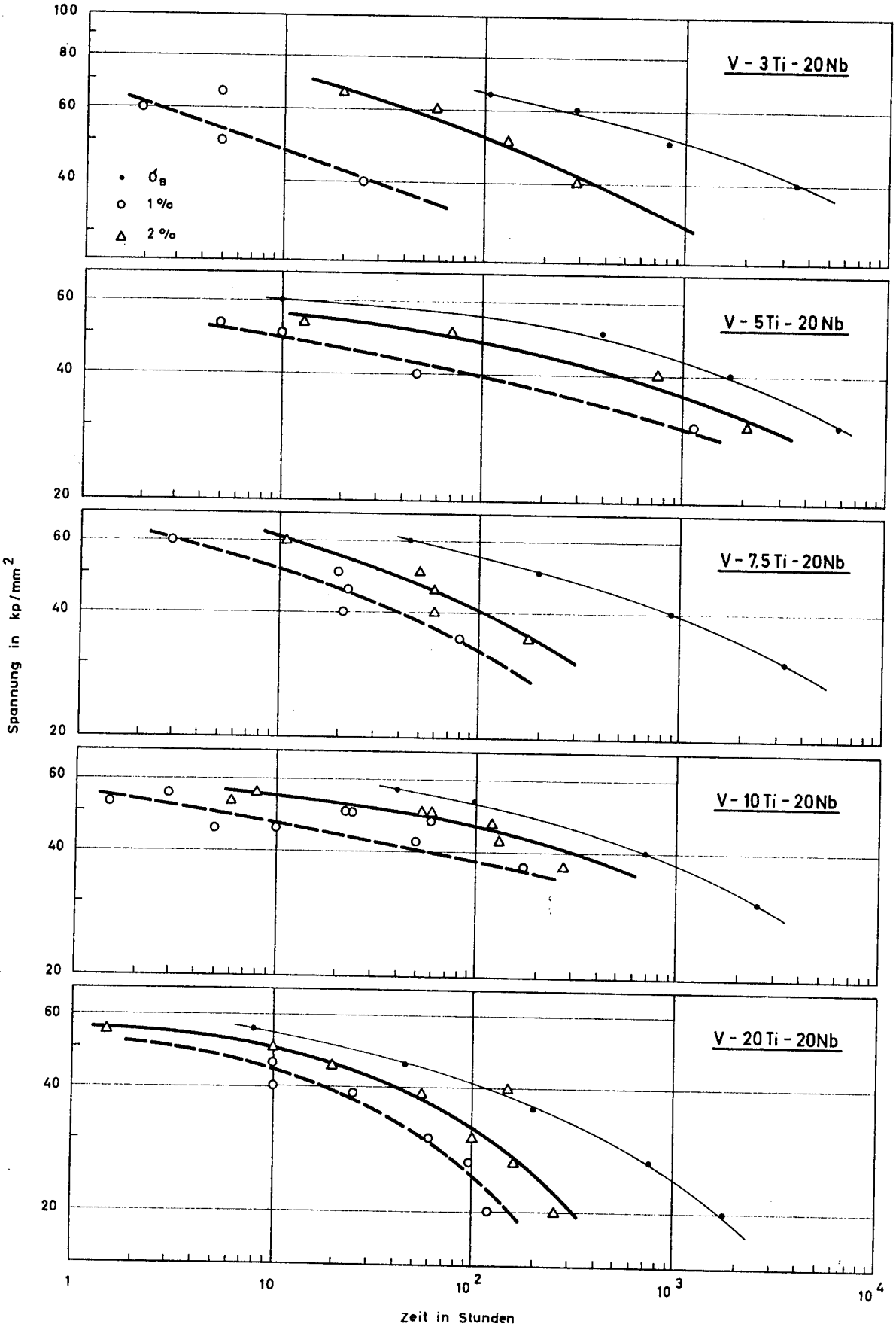

Bild 29 : Zeit - Dehngrenzen in Abhängigkeit von der Spannung T = 650 °C
P ≈ $1 \cdot 10^{-5}$ Torr

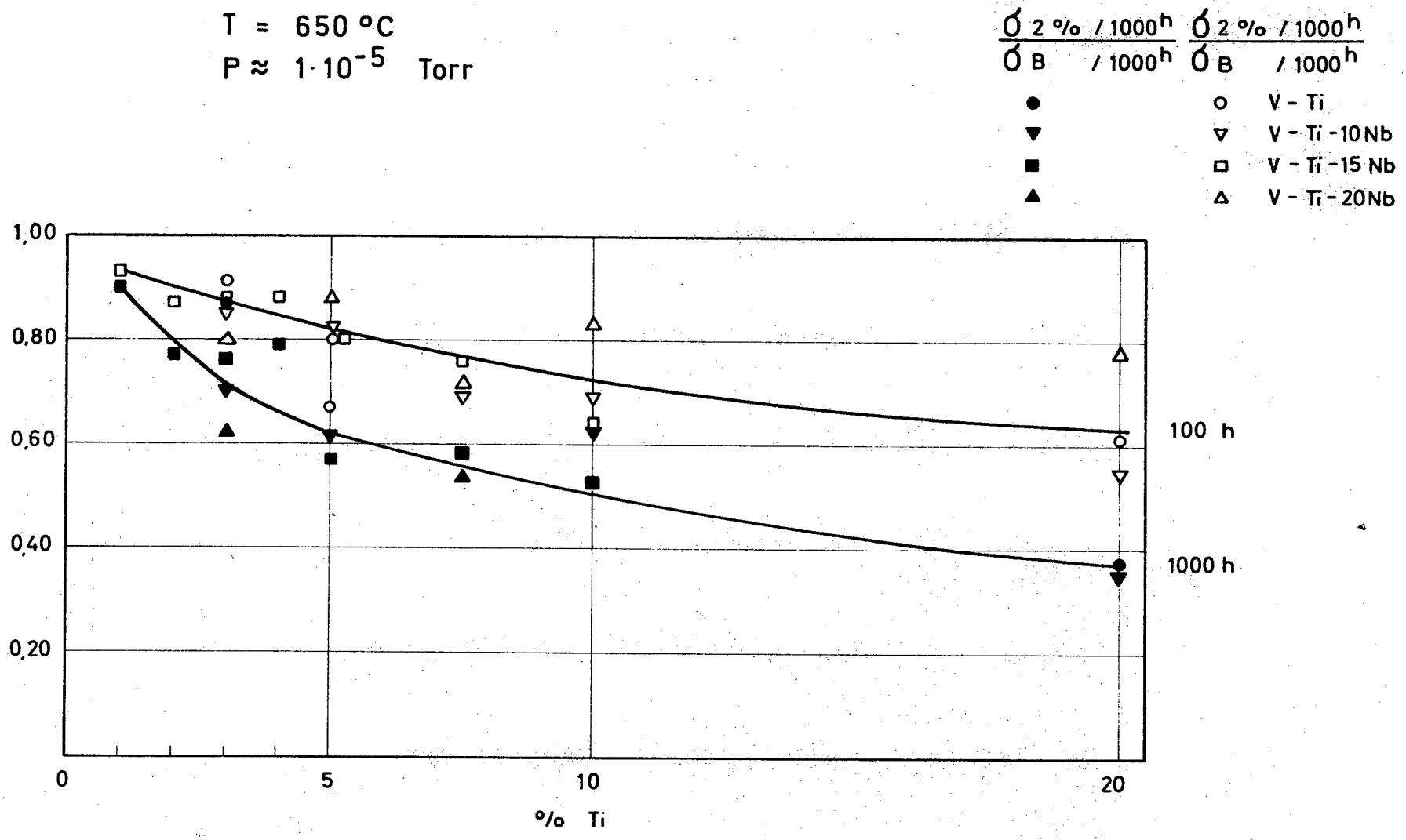

Bild *30*: Verhältnis Zeitdehngrenze zu Zeitstandfestigkeit in Abhängigkeit vom Ti - Gehalt für 2 % Dehnung bei 100 h bzw. 1000 h Standzeit

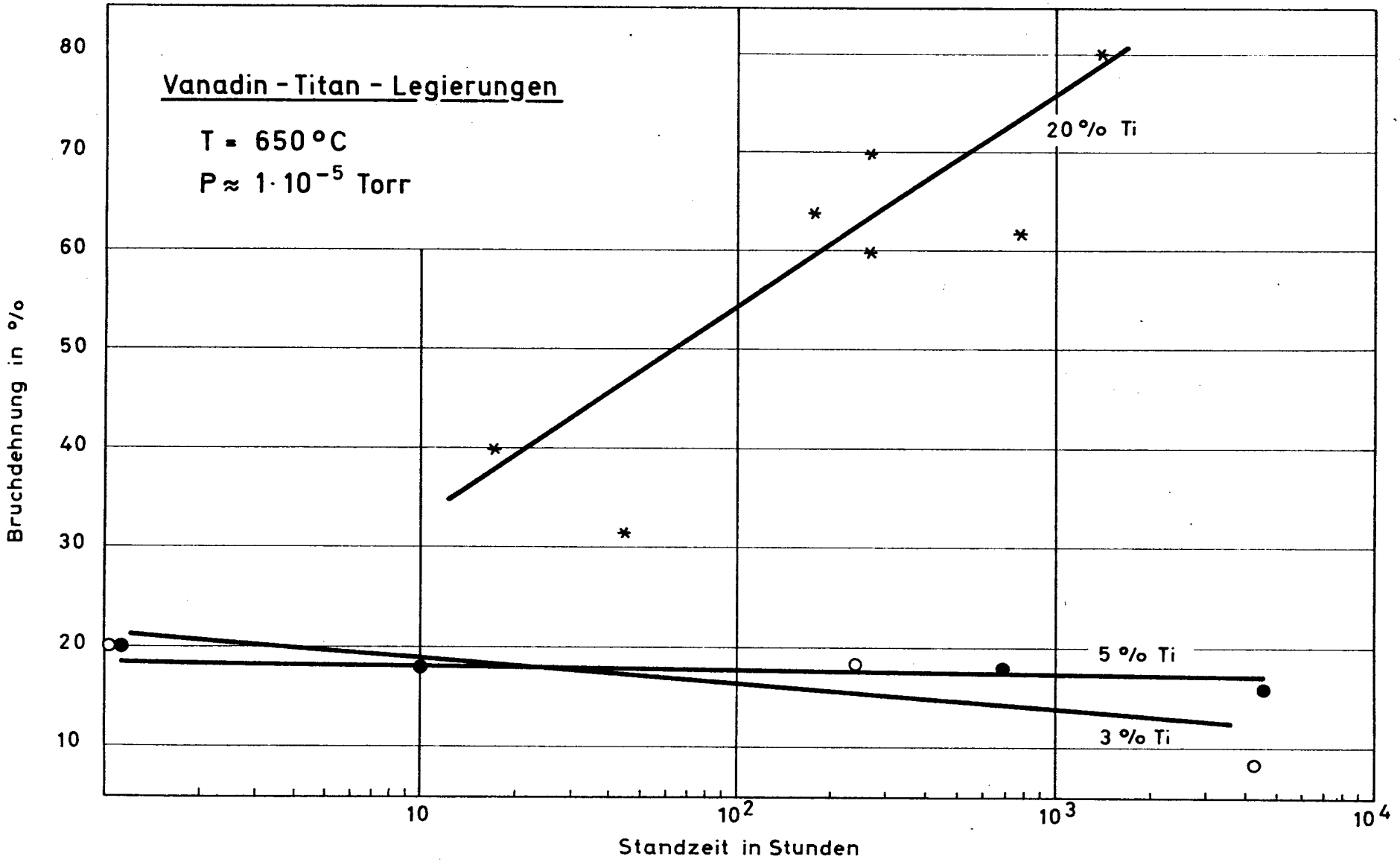

Bild 31 : Bruchdehnung in Abhängigkeit von der Standzeit bei verschiedenen Ti - Gehalten

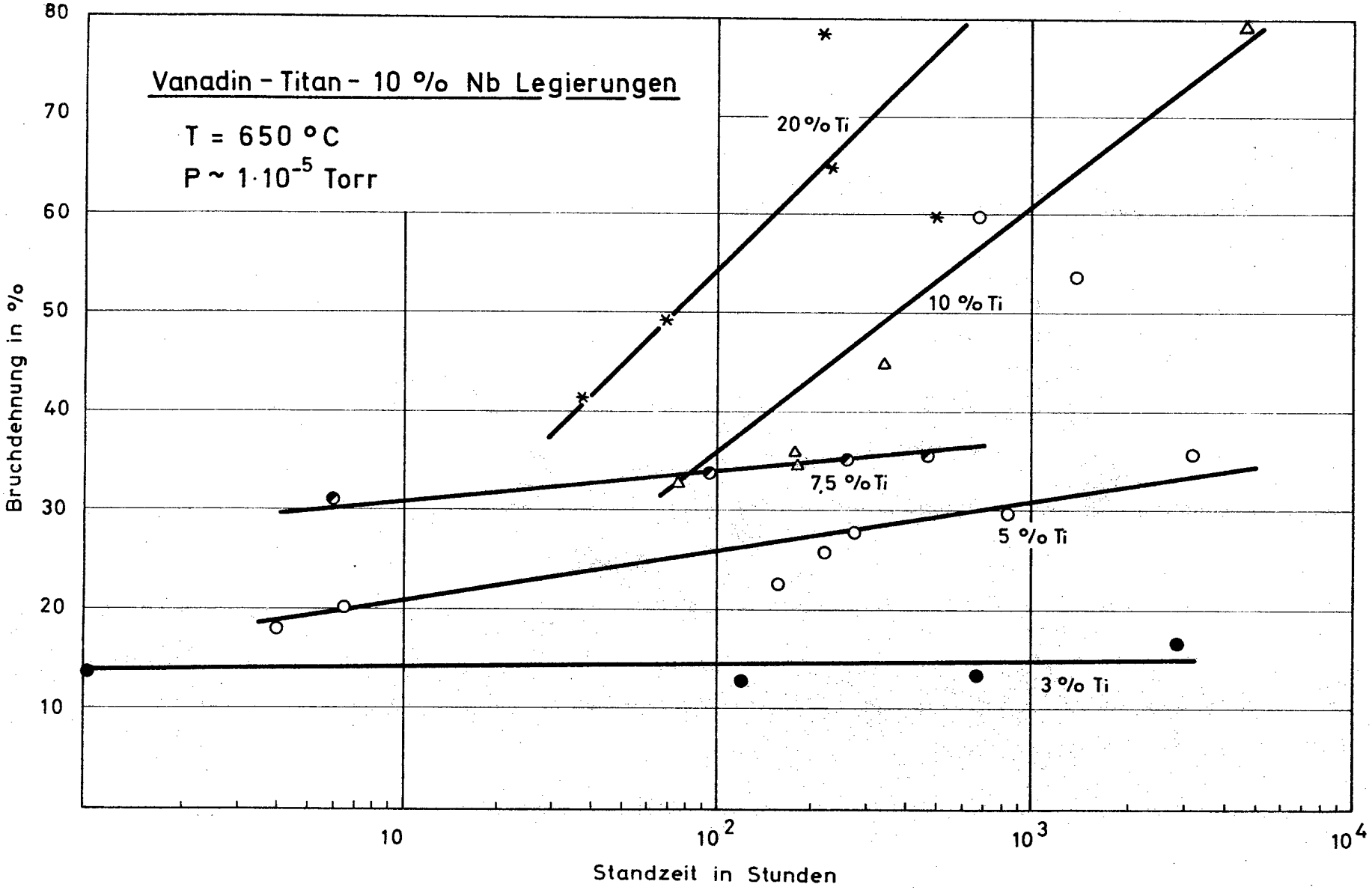

Bild 32: Bruchdehnung in Abhängigkeit von der Standzeit bei verschiedenen Ti-Gehalten

Bruchgefüge

V-2Ti-15Nb

T = 650°

σ = 40 kp/mm²

t_B = 6328 Std.

HV_{30} = 227-235

V-5Ti

T = 700°C

σ = 10 kp/mm²

t_B = 6630 Std.

HV_{30} = 138-145

x 100

Bruchgefüge

V-3Ti-20Nb

T = 850°

σ = 6 kp/mm^2

t_B = 2078 Std.

HV_{30} = 215-244

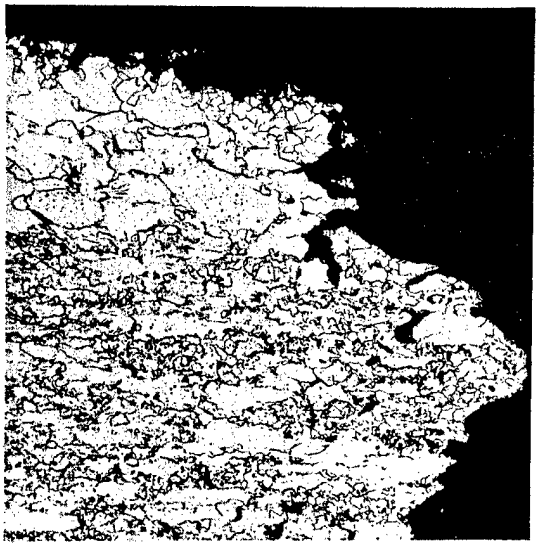

V-3Ti-15Nb

T = 920°

σ = 4 kp/mm^2

t_B = 188 Std.

HV_{30} = 194-198

x 100

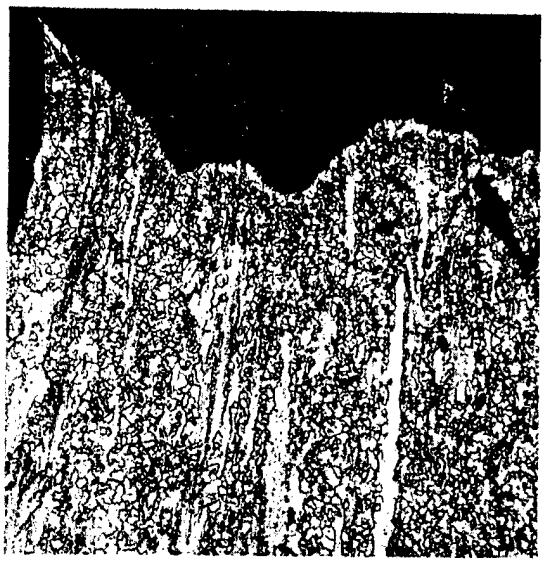

V-3Ti-20Nb

T = 850°C

σ = 6 kp/mm^2

t_B = 2078 Std.

δ_{sd} = 123%

Bruchzone

HV_{30} = 215-244

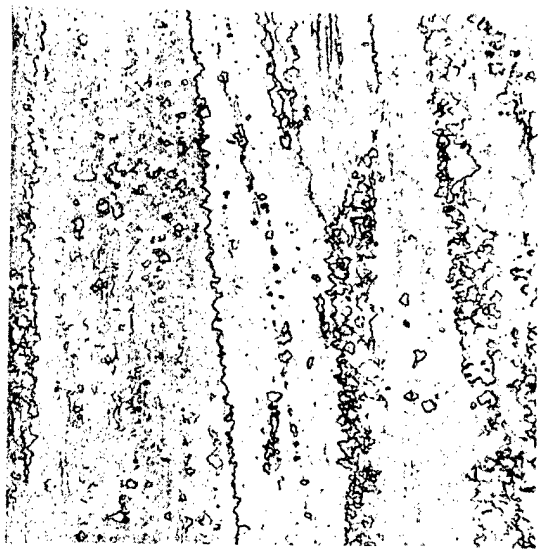

Meßlänge

Kopf

HV_{30} = 210-224

These photographs reduced 10% in printing process.

x 100

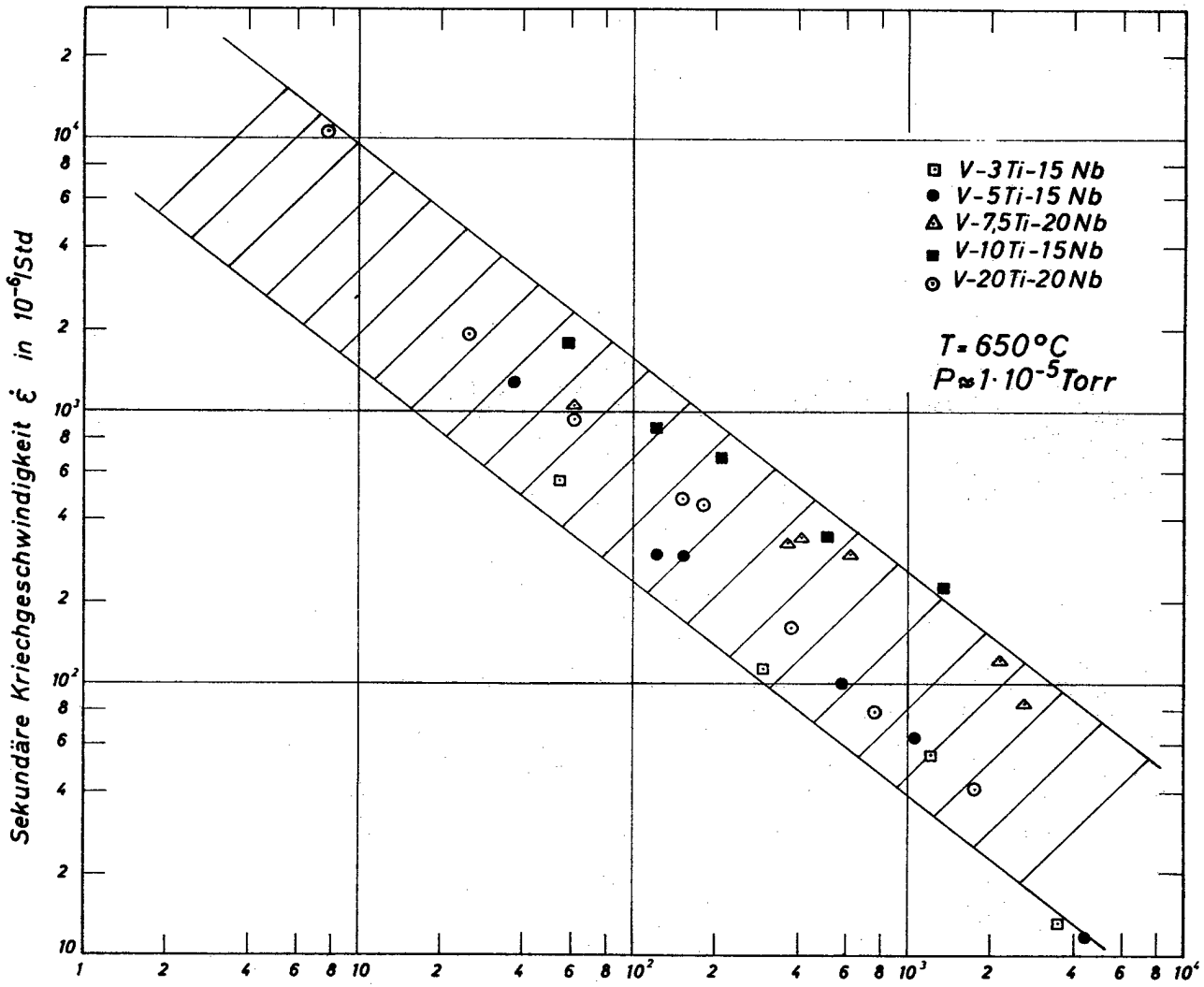

Bild 36: Sekundäre Kriechgeschwindigkeit in Abhängigkeit von der Standzeit